Zhou, W., Minnick M. D., and Cui, C. (2018) GIS for Natural Resources (Mineral, Energy, and Water). In: Huang, B. (Ed.), Comprehensive Geographic Information Systems Vol. 2, pp. 158–186. Oxford: Elsevier. ISBN: 9780128046609 https://doi.org/10.1016/B978-0-12-409548-9.09643-3

GIS for Natural Resources (Mineral, Energy and Water)

Wendy Zhou[1*], Matthew D. Minnick[2], and Celena Cui[1]

[1] Department of Geology and Geological Engineering, Colorado School of Mines
1516 Illinois St. Golden, CO 80401
Email: wzhou@mines.edu

[2] RESPEC Inc
4614 West Main St.
Rapid City, SD 57702

Abstract/Synopsis

Natural resources embrace a broad array of categories, including agricultural, conservational, forestry, oceanic, water, energy, and mineral resources. This chapter only focuses on the latter three. Traditional methods for natural resource management include, but are not limited to, geophysical exploration, field geological mapping, geochemical analysis, and aero-photo interpretations. Natural resource related research is by nature a spatial problem. Integration of field survey data and other pertinent information can be a time-consuming task by traditional ways. With the help of GIS, most of the tasks can be conducted in ways that are nearly impossible in traditional methods. Three case studies of GIS application in natural resource analyses will be presented in this book chapter to demonstrate the GIS applications in compiling, integrating, analyzing and visualizing natural resource data.

Keywords

Geodatabase, Geospatial infrastructure, Oil shale, 3D geologic model, Onsite wastewater treatment system, Nitrogen fate and transport, Groundwater, Advection–dispersion, Aquifer vulnerability, Placer gold, Offshore mineral resources; Resource estimate

1.0 Introduction

Natural resources embrace a broad array of categories, including agricultural, conservational, forestry, oceanic, water, energy, and mineral resources. This chapter only focuses on the latter three. The process of natural resource development includes resource exploration, resource assessment, resource management, and resource production. Traditional methods for natural resource exploration include, but are not limited to, geophysical exploration, field geological mapping, geochemical analysis, and aero-photo interpretations. Integration of field survey data and other pertinent information for the purpose of natural resource estimation can be a time-consuming task by traditional methods. Natural resource related research is by nature a spatial problem. With the help of Geographic Information Systems (GIS) technology, most of the tasks related to natural

resource development can be conducted in ways that are nearly impossible with traditional methods. With the digital mapping capacity of GIS and the ever-evolving functionalities of GIS in recent decades, the industry has shifted to using GIS as the preferred tool for resource exploration, planning, analysis, visualization, and management. Moreover, the state and federal agencies involved in the natural resource management and environmental regulating process are adopting the GIS format as the standard for communicating spatial data in digital format (Bonham-Carter, 1996; Price, 2001).

The development of GIS has a long history. One of the important milestones of GIS history is the creation of the Canada Geographic Information System (CGIS), the First National GIS System, in 1964. Since then GIS became a powerful time-efficient and cost-effective technique for miners, geologists, scientists and engineers who have been solving problems related to geo-spatial data in traditional way for generations. There are many different definitions of GIS, for example, the United State Geological Survey (USGS) defines GIS as a computer system capable of assembling, storing, management, analyzing, and displaying geographically referenced data, i.e. geo-spatial data identified according to their locations (USGS, 2007). GIS Experts also look the total GIS as including operating personnel and the data that go into the system.

GIS has been used in managing and archive large volume of natural resource data. A good is example of such a data management system is the USGS Mineral Resources Data System (MRDS). MRDS is a collection of reports describing metallic and nonmetallic mineral resources throughout the world. Included are deposit name, location, commodity, deposit description, geologic characteristics, production, reserves, resources, and references. GIS is an ideal platform to bring data in heterogeneous formats together and deliver meaningful information. GIS can also be used to integrate survey data with block models or mine design data from other software packages such as GeoSoft, Vulcan, MineSight, SURPAC Range, or Mining Visualization System (MVS) (ESRI, 2006).

There are many examples of GIS applications in natural resource management. The literatures cited here are not intending to be a complete bibliography list; rather it gives examples of the GIS applications in natural resource management. For instance, Wing and Bettinger (2008) wrote a book on GIS application in Natural resource management which is an introductory text book for college students majoring in forestry and natural resource management, field forestry, biology, and other natural resource or natural resource-related fields. An example given by ESRI (ESRI, 2006) is the GIS application in building a virtual three-dimensional (3D) GIS model for Mayflower Gold Mine in southwest Montana. Hammond (2002) showed an example of GIS application in an underground mining, which focused on four areas: land ownership and mineral claims, exploration management, production, and mine safety. Berry and Pistocchi (2003) presented an application of GIS, together with multi-criteria analysis for supporting decision making, in the environmental impact assessment of open-pit quarries. Dillon and Blackwell (2003) conversed in general about GIS application in surface mining development. Starting from the exploration database, their paper described how a GIS

can be used for the development of mining plans based on topography, geology and mineralization information stored in a relational database. The Application of GIS to Bauxite Mining in Jamaica (Almarales–Hamm, et al., undated) is an example of GIS applications supported by satellite imagery and orthorectified aerial photography to manage, analyze, and display data on tonnage, ore quality, location, and ownership. A customized 3D modeling and mine planning system using ArcGIS and its extensions provide tools that assist in the decision making process and reserve management. Water is one of the most precious nature resources on the Earth. GIS applications in water resource study embraces a broad spectrum of topics, ranging from hydrological cycle, hydrologic processes modeling (e.g. Naiman et al., 1997; National Research Council, 1999), watershed characterization, assessment of environmental condition of water catchments (e.g. Aspinall and Pearson, 2000; Di Luzio et al., 2004), as well as water resource assessment in both quality and quantity (e.g. Cui et al., 2016; Zhou et al., 2015). Additionally, Wilson et al. (2000) examined the advancement of water resource assessment and management by integrating GIS and hydrological simulation model. GIS has also been used intensively in both conventional and unconventional fossil energy resource assessment and management. For instance, the USGS energy resource program did outstanding works in assessment of in-place oil shale resources in the Green River Formation (Johnson et al., 2011; Mercier, et al., 2011a, 2011b; Mercier 2011; Self et al., 2011; Brownfield et al., 2011). Their works demonstrated GIS applications in in-place resource assessment and overburden calculation.

Using mineral resource as an example of natural resources, Zhou (2009) summarized the GIS applications for mining industry as followings:

1). Pre-production phase of a mine
   a. Site selection
   b. Land ownership
   c. Mineral claims
   d. Exploration management
2). Applications of GIS to the production phase of a mine
   a. Environmental Quality Monitoring
   b. Facilities Management
   c. Volume Computations
   d. Emergency management and industrial security
   e. Transport routes
3). Applications of GIS to the post-production phase of a mine
   a. Reclamation, Vegetation Characterization
   b. Slope-Aspect Characterization
   c. Volume Computations
   d. Visualization
4). GIS –based analysis method for technical research in field of mineral and mining
   a. Resources estimation
   b. Environmental impact assessment

In the following sections, three comprehensive case studies in the subjects of GIS applications in natural resource and environmental assessment will be presented. The first study is an example of GIS Application in water resource geospatial infrastructure development for supporting oil shale development in Piceance Basin, Northwestern Colorado. The second study describes a GIS application in assessment of surficial groundwater aquifer vulnerability for the State of Florida. The last study presents an example of placer gold mine in-place resource estimation in Nome, Alaska. This chapter is a synthesis of a series of previously non-published and published works. Through all case studies, GIS technology has been applied to compile, integrate, analyze and visualize natural resource data in two-dimensional or three-dimensional domains. It is demonstrated that GIS-based analyses have helped for making informed decisions and for revealing or discovering new information or knowledge in ways that are impossible by using conventional methods alone.

2.0 GIS Application in Water Resource Geospatial Infrastructure Development for Supporting Oil Shale Development in Piceance Basin, Northwestern Colorado, USA

2.1 Background

Large oil shale deposits are found throughout the Midwestern and Eastern United States. However, the deposits of the Green River Formation in northwestern Colorado, southwestern Wyoming, and northeastern Utah (Figure 1) are most likely to be developed because of their richness, accessibility, and extensive prior characterization (USGS, 2005). Development of oil shale resources in Western U.S. will require significant quantities of water for oil shale retorting, reclamation, and associated economic growth. The current water consumption estimation, based on retorting methods from oil shale industry, is of 3:1 water-to-oil ratio (Wood et al., 2008). For an oil shale industry producing 2.5 million barrels of oil per day, this equates to between 105 and 315 million gallons of water per day for power generation for in-situ heating processes, retorting, refining, reclamation, dust control and on-site worker demands.

Collecting regional “baseline” data and compiling them into an integrated database is the groundwork of addressing potential water issues due to oil shale development on a regional basis (NETL, 2007). The current methods used in collecting and storing oil shale related data overwhelm our current ability to make these valuable data resources easily available to both the scientific community and policy-makers. Despite different levels of technical knowledge, the data consumers face similar problems of locating, assembling, and integrating heterogeneous domain-specific data into a format that meets their needs. This task could be possible for the technically savvy data

Zhou, W., Minnick M. D., and Cui, C. (2018) GIS for Natural Resources (Mineral, Energy, and Water). In: Huang, B. (Ed.), Comprehensive Geographic Information Systems Vol. 2, pp. 158–186. Oxford: Elsevier. ISBN: 9780128046609 https://doi.org/10.1016/B978-0-12-409548-9.09643-3

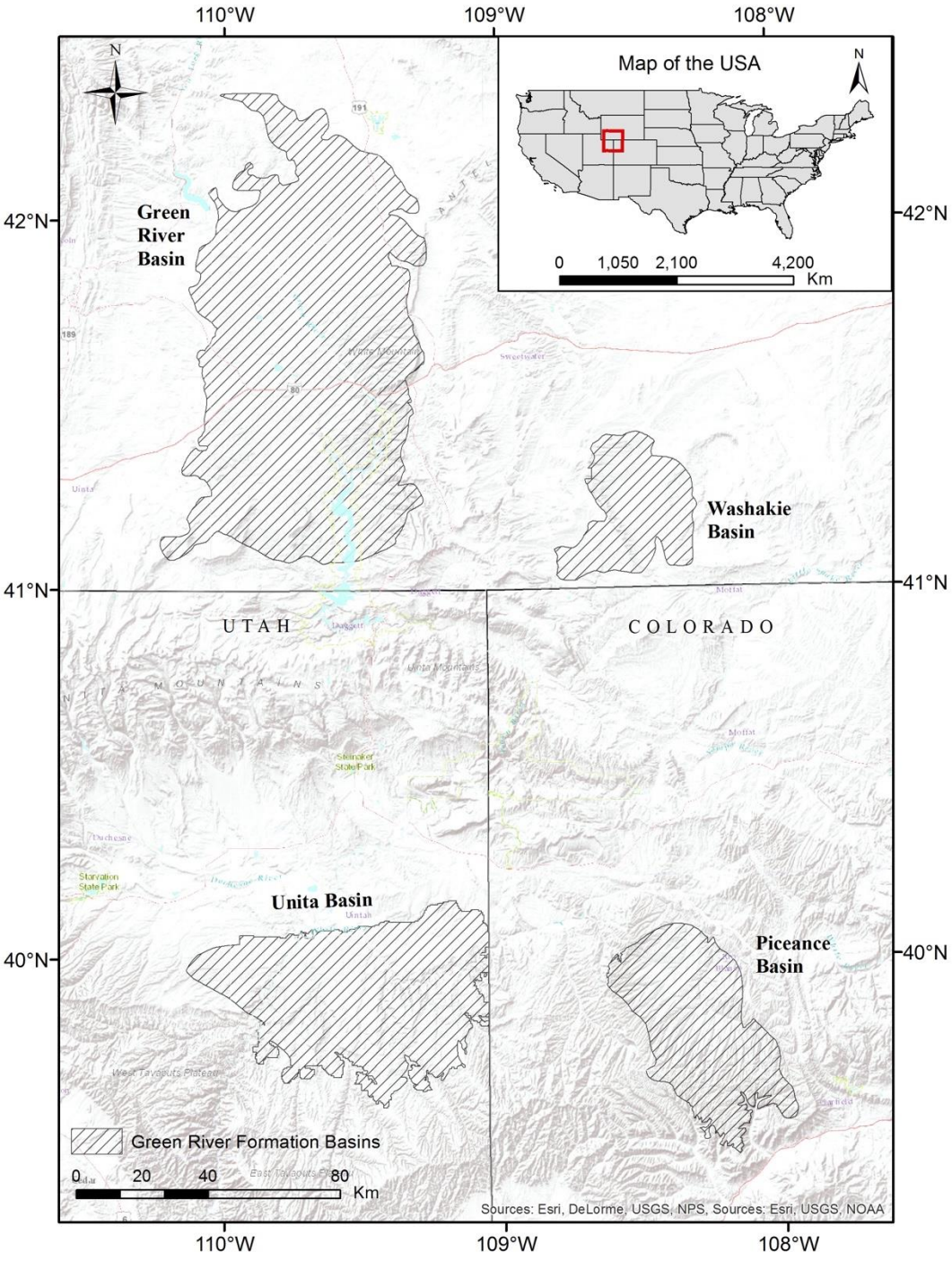

Figure 1. The locations of four Green River Formation basins (in upright diagonal fill pattern) in Colorado, Utah, and Wyoming (Zhou et al., 2015).

consumer, but often only with significant and time-consuming effort that could be better spent on data analysis. The ability to view products based on multiple heterogeneous datasets in a new and novel manner is often the key to enhancing scientific understanding.

Among all the Green River Formation basins, the Piceance in northwestern Colorado has the smallest area but largest resource (Johnson et al., 2011). Hence, the Piceance Basin was selected as the study area. USGS has done intensive works in assessment of in-place oil shale resources in the Green River Formation. Readers, who are interested in the formation and evolution of these oil-shale basins and the assessment of in-place oil shale resources in the Green River Formation, please refer to a series of publications by the USGS Oil Shale Assessment Project: Oil Shale Resources of the Eocene Green River Formation, Greater Green River Basin, Wyoming, Colorado, and Utah lead by Ronald C. Johnson (Johnson et al., 2011; Mercier, et al., 2011a, 2011b; Mercier 2011; Self et al., 2011; Brownfield et al., 2011).

In this project, our research focused on building a GIS-based water resource geospatial infrastructure for data storing, managing, manipulating, modeling, visualizing, and integrated the infrastructure with 3D geologic, system dynamic and surface water resource analysis models. Study of water availability and environmental impact is a critical early step for the potential development of oil shale resources in the Western U. S. The ultimate goal of this study is to provide supporting information for water resources assessment and for better decision making on oil shale resource development in the Western U. S., as well as for facilitating environmental impact studies. Research protocols developed in this study were based on Piceance Basin, but intended to be general so that they can be readily adapted to other similar study areas.

The sections will present the research project of GIS application in water resource geospatial infrastructure development for supporting oil shale development in Piceance Basin, Northwestern Colorado. This presentation is a synthesis of previously published or unpublished works by a multi-institutional research group lead by the Colorado School of Mines, joined by Idaho National Laboratory, University of Texas San Antonio, and Oklahoma Geological Survey (Zhou, et al., 2012, 2015; Mattson et al., 2012). The presentation of this project will start with data collection and integration, followed by 3D geologic model and analytical models in support oil Shale development, and ended with results and summary.

2.2 Baseline Data Collection and Integration

Data collected and compiled include a Microsoft Access database containing Fischer assays of oil shale drill cores for the Piceance Basin created by the USGS Oil Shale Assessment Team, the National Hydrography Dataset Plus (NHD Plus), 10-meter digital elevation model (DEM), geologic maps, subsurface geology, land use dataset, vegetation classification data, stream flow, precipitation, climate, well, ground water level, water use, water right data, and water quality data. Water quality data were

collected from the USGS National Water Information System (NWIS) and the United State Environmental Protection Agency (US EPA) STOrage and RETrieval (STORET) Data Warehouse. Locations for 893 springs were collected from the Colorado Decision Support System (CDSS). Table 1 summarizes various data collected, data sources and brief descriptions of the data (Zhou, et al. 2012; Zhou, et al., 2015).

The 1:100,000 scale geologic quadrangle maps (Hail and Smith, 1994; 1997) of the Piceance Basin were obtained from USGS in DJVU format and were georeferenced into ArcGIS compatible image. Two major products, surface expression of faults and surficial alluvial deposits, are georeferenced and digitized from the USGS 100:000 scale geologic maps for the Piceance Basin and added to the "baseline" geodatabase.

Additional data are searched from the *Tell Ertl Oil Shale Repository* (TEOSR) at the Arthur Lakes Library of Colorado School of Mines after readily available digital resources were exhausted. The TEOSR contains materials related to oil shale and the history of the oil shale industry. Technical materials include journals, government, contractor reports, and unpublished papers of key oil shale players, original research maps, charts, and data compilations.

Table 1. Summary of data acquisition for Piceance Basin

NAME	SOURCE	DESCRIPTION	GEODATABASE FEATURE
Watersheds (HUCS)	NHDplus	Watershed polygons at various scales from the National Hydrologic Dataset	Basin Feature Class
Elevation	NED	Digital Elevation Models 90m, 30m, and 10m from the National Elevation Dataset	GeoRasters
Catchments	NHDplus	Lowest level of surface water divisions defined by the Stream Networks from the National Hydrologic Dataset	Catchment Feature Class
Stream Networks	NHDplus	Stream line data networked in a reach and nodal system from the National Hydrologic Dataset	Hydroline Feature Class
Flow Accumulation	NHDplus	Flow network and direction data linked to the Stream Network from the National Hydrologic Dataset	Related Table
Flow Gages	CDSS, NWIS	USGS Flow Gage Point Locations	Monitoring Point Feature Class
Flow Data	NWIS	Time Series Stream Flow Data linked to Flow Gage ID	Time Series Table
Daymet Extraction Points	Centroid of WARMF model catchments	Points calculated at centroids of WARMF model catchments for Daymet data extraction	Custom Point Feature Class

Precipitation Data (Time Series)	Daymet	Time Series Precipitation Data from Daymet linked to monitoring stations, processed yearly, and monthly precipitation data trends for watersheds	Time Series Table
Meteorologial Data (Time Series)	Daymet	Time Series Temperature Data and processed Temperature Datasets from Daymet	Time Series Table
Climate Monitoring Stations	NOAA, CDSS	Point locations for Climate Monitoring Stations in and around the Piceance Basin	Monitoring Point Feature Class
Climate Monitoring Stations	NOAA	Downloaded time series for up to 55 climate/weather parameters	Time Series Table
Surface Water Quality	NWIS, EPA STORET	Water Quality Data linked to monitoring locations	Monitoring Point Feature Class
Aerial Imagery	USGS, NAIP, ESRI Services	Color Aerial Imagery at varying resolutions	Raster Catalog
Geologic Maps	CGS, USGS	Images of geologic maps at various scales, georeferenced, from the CGS and USGS	GeoRasters and GeoArea feature class
Subsurface Geology	USGS, CSM Database	Borehole data from exploration wells including geophysical data, formation tops, oil shale richness data Input for 3D Geologic Model	GeoVolume Multipatch Feature Class
Wells	NWIS	Water Wells with production and source data	Well Point Feature Class
Water Level Data	NWIS	Time Series Data of Water Level Measurements for Wells	Time Series Table
Ground Water Quality	NWIS	Water Quality Data Associated with Wells	Time Series Tables
Hydrogeologic Data	CGS, USGS	Hydrologic Parameter data derived from cores and pumptests	Tables
Land Cover	NLCD	Vegetation and Barren Land Data from the National Land Cover Dataset	Raster Feature Set
Land Use Ownership	BLM	Land Use and Ownership Data	Custom Polygon Feature Class
Base Map Layers	USGS, ESRI Services	General map data including roads, towns, population, site names, USGS topographic maps	ESRI Services not Included in Geodatabase
Springs	CDSS	Point Data for Locations and Time Series Tables for Flow	Hydro Point Feature Class
Spring Flow	CDSS	Time Series Data of Water Flow from Springs	Time Series Tables

Diversions	CDSS	Irrigation Ditches, Stock Ponds, Reservoirs, Stream Pumping Locations and Wells	Water Discharge and Water Withdraw Point Feature Classes
Diversion Flow	CDSS	Time Series Data of Water Flow and Usage	Time Series Tables
Pumping Tests	TEOSR	Testes conducted by various institutions throughout the years compiled from non-digital documents	Point Feature Class
Surficial Geological Structure	Digitized from USGS Geologic Map	surface expression of faults in Piceance Basin	Polyline Feature Class
Surficial Alluvial Deposits	Digitized from USGS Geologic Map	surficial alluvial deposits that make up the stream valleys in the Piceance Basin	Polygon Feature Class

Database is strictly defined as one or more structured sets of persistent data, managed and stored as a unit and generally associated with software to update and query the data (Litton, 1987; Navathe and Elmasri, 2002). A geodatabase is a collection of geographic datasets for use by ArcGIS (Date, 2003; ESRI 2004a), and can include the spatial locations and shapes of geographic features recorded as points, polylines, polygons, pixels, or grid cells, as well as their attributes and relationships among them (Date, 2003). The geodatabase format in ArcGIS functions is similar to any relational database management system (RDBMS). Data retrieved from various sources are integrated via the geodatabase format into an integrated geodatabase as shown in Figure 2. The integrated geodatabase is capable of performing basic and advanced GIS operations, such as queries, and spatial, geostatistical and 3D analyses, allows one to perform surface creation, multipatch creation and multicriteria decision analysis tasks.

Arc Hydro, the current industry standard relational database for water resource analysis on the ArcGIS platform, was chosen as the database schema for the prototype database framework. Arc Hydro has two separate geodatabase schemas, one to support surface water datasets and the other to support groundwater datasets. The Arc Hydro framework supports a toolbar and a geoprocessing toolbox in ArcGIS for data analysis and simple modeling (Maidment, 2002). The surface water and groundwater databases were built separately at the early stage of the project because it allows us to better manage the data and avoid duplication of effort, and were then broken down into basic components and rebuilt into one geodatabase. The data schema was customized to support generating the input data of the surface water and the system dynamic models. The definition of the database schema was accomplished by selecting a “data model” on which the project geodatabase was based. A “data model” is the representation of a real world phenomenon or system within a database with a conceptually logical framework. When designing a data model, the main features of the system must be defined using geographic features, tabular data and relationships between those features as cardinality or topological relationships. A well designed model or data model allows for efficient analysis of the system behavior. The Arc Hydro Data Model (AHDM) was selected as the database schema for this project because it supports the fundamental data types used

in this project while being extensible, flexible, and adaptable to our modeling and web-based applications in the meantime.

As mentioned above, we elected to build two separate databases at the early stage of the project: An Arc Hydro Surface Water (AHSW) geodatabase, and an Arc Hydro Ground Water (AHGW) geodatabase. The two databases were integrated into one with the evolvement of the project. The basic framework of the overall geospatial infrastructure is represented in Figure 2, which shows the relationship between the databases and the analytical models. An ArcGIS geodatabase schema is summarized in Figure 3 for the implementation of the integrated database.

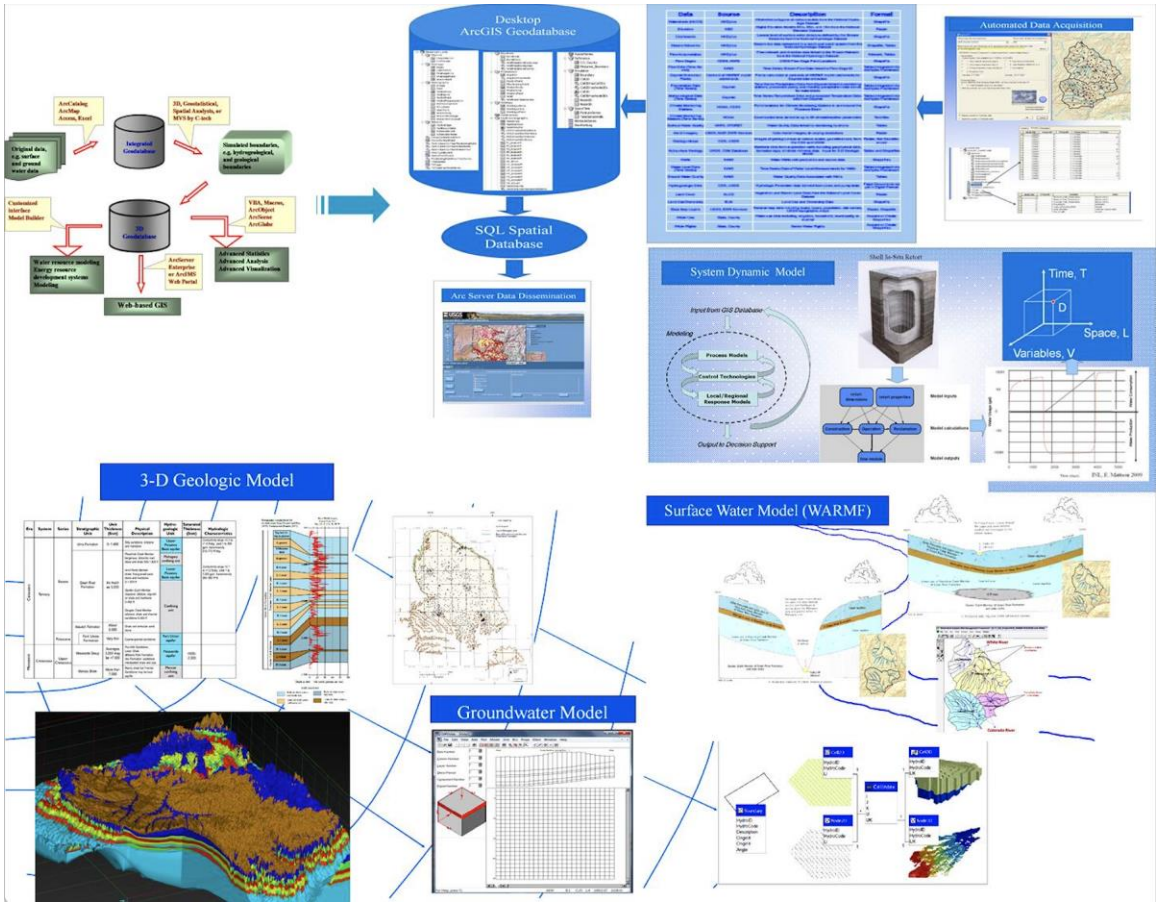

Figure 2. The high-level geospatial infrastructure

Zhou, W., Minnick M. D., and Cui, C. (2018) GIS for Natural Resources (Mineral, Energy, and Water). In: Huang, B. (Ed.), Comprehensive Geographic Information Systems Vol. 2, pp. 158–186. Oxford: Elsevier. ISBN: 9780128046609 https://doi.org/10.1016/B978-0-12-409548-9.09643-3

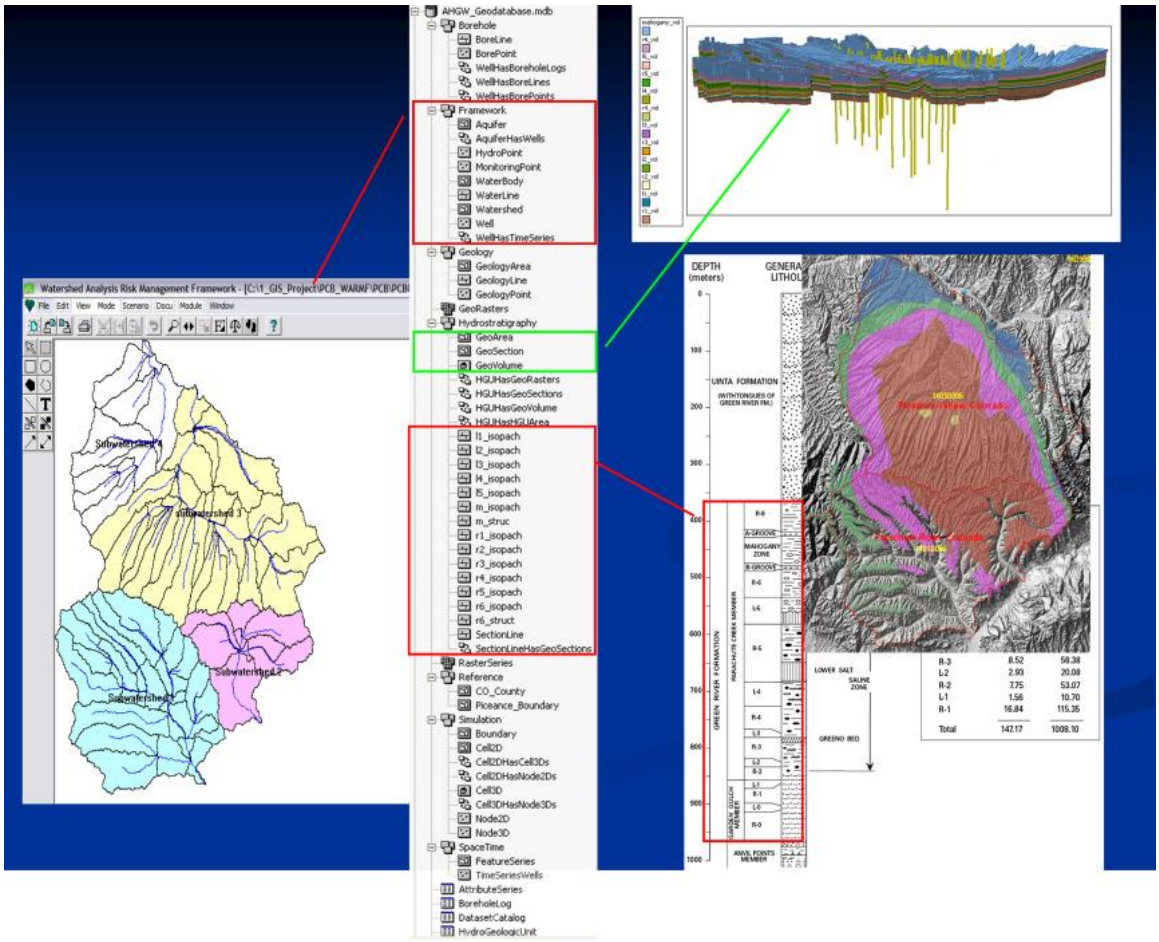

Figure 3. The ArcCatalog tree of the integrated database partially shows the structure of the database, such as file geodatabase tables, relationship classes, feature datasets, and rasters (Zhou et al., 2015)

2.3 Analytical Models in Support of Oil Shale Development

Four analytical models, namely three-dimensional (3D) geologic, and system dynamic, surface water, and groundwater models, were developed for this project. The centralized geospatial infrastructure served as the groundwork for setting up the frameworks for these analytical models. Such a centralized geospatial infrastructure made it possible to directly generate model inputs from the same database and to indirectly couple the different models through inputs/outputs. In this book chapter, we only focus on presenting the 3D geologic and system dynamic models. Readers who are interesting in the surface water and ground water models, please refer to Zhou et al. (2012; 2015).

2.3.1 Three-dimensional (3D) Geologic Modeling

Zhou, W., Minnick M. D., and Cui, C. (2018) GIS for Natural Resources (Mineral, Energy, and Water). In: Huang, B. (Ed.), Comprehensive Geographic Information Systems Vol. 2, pp. 158–186. Oxford: Elsevier. ISBN: 9780128046609 https://doi.org/10.1016/B978-0-12-409548-9.09643-3

3D visualization and volume calculation are essential for in-place nature resource evaluation. A fully attributed 3D geologic model of the Piceance Basin was built to support groundwater, and system dynamic modeling. The 3D geologic model consists of, from top to bottom, Uinta, Upper Green River, Lower Green River, Wasatch and Mesaverde Formations. The oil sale-bearing Lower Green River strata were separated into alternating layers of oil-rich zones (R-zones) and oil-lean zones (L-zones) following the name convention from Cashion and Donnell (1972) and Self et al. (2010). There are sixteen layers in the Lower Green River Formation. These are, from top to bottom, A-groove, Mahogany, B-groove, R-6 Zone, L-5 Zone, R-5 Zone, L-4 Zone, R-4 Zone, L-3 Zone, R-3 Zone, L-2 Zone, R-2 Zone, L-1 Zone, R-1 Zone, L-0 Zone, and R-0 Zone. The input data for the 3D geologic model mainly included the USGS Fischer Assay (Mercier et al., 2009), Geologic Tops data, and a 10-meter Digital Elevation Model (DEM).

In order to make sure the surface interpolations were reliable, a lengthy process of model quality assurance/quality control (QA/QC) was conduct to correct geometric inconsistency issues in the model. Each interpolated surface was singled out. Data distribution and resulting structure representation were then verified. When necessary, additional data points were added to an interpolated surface to fill out missing sections of the original data and maintain consistency in the geometric structure and average layer thickness in the neighborhood. Figure 4 shows the final top surface after QA/QC for the Mahogany Zone of the Green River formation. The digitized structure information from USGS geologic maps is overlain on the surface interpolation to verify consistency in the layers. The QA/QC process was done for all interpolated surfaces in the model. After all the interpolated surfaces were verified, a full basin scale model was reconstructed at various grid resolutions (Figure 5). Once this was completed, cross sections could be extracted from the model and exported to a 3D geospatial dataset in the project database. These layers and cross sections can be served out via ArcGIS service and accessed through ArcExplorer (Figure 6).

The Mining Visualization Systems (MVS) software by C-Tech was chosen for building the 3D geologic model due to the nature of the data and its compatibility with ArcGIS. MatLab scripts were written to process the raw assay and geologic tops data from the USGS geospatial database into MVS input files to facilitate advanced visualization and interpolation of the data set.

Zhou, W., Minnick M. D., and Cui, C. (2018) GIS for Natural Resources (Mineral, Energy, and Water). In: Huang, B. (Ed.), Comprehensive Geographic Information Systems Vol. 2, pp. 158–186. Oxford: Elsevier. ISBN: 9780128046609 https://doi.org/10.1016/B978-0-12-409548-9.09643-3

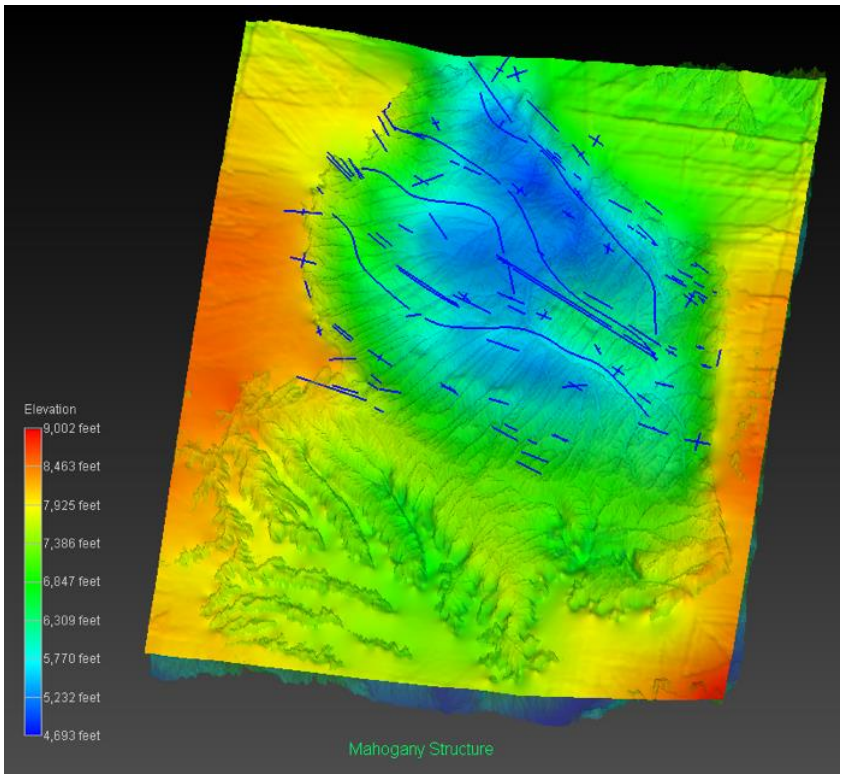

Figure 4. Image of the top of Mahogany surface in the Green River Formation colored by elevation reveals the layer structure which is verified via the USGS structural interpretations.

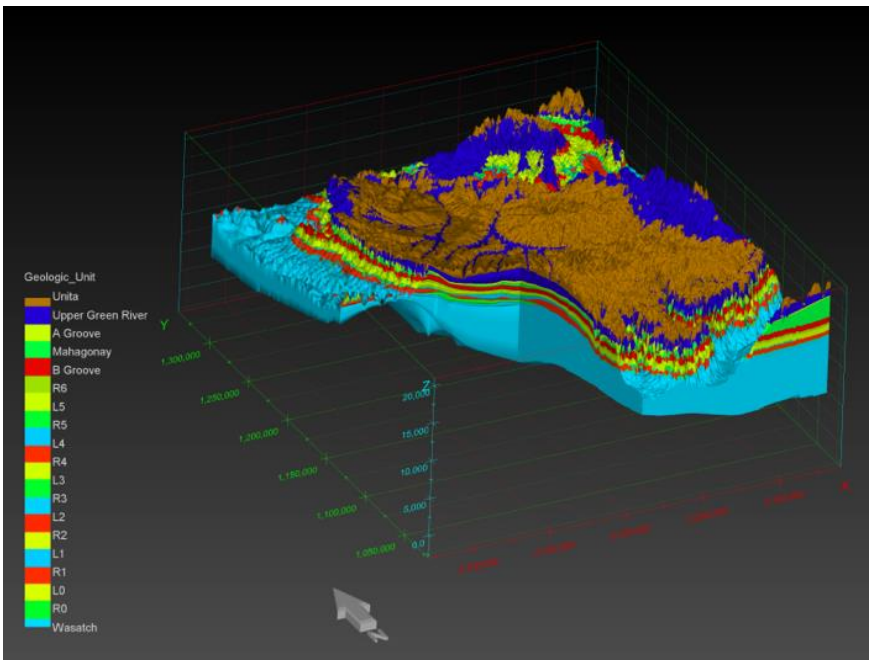

Figure 5. Output of a basin wide 3D geologic model post QA/QC with a vertical exaggeration of 10 times.

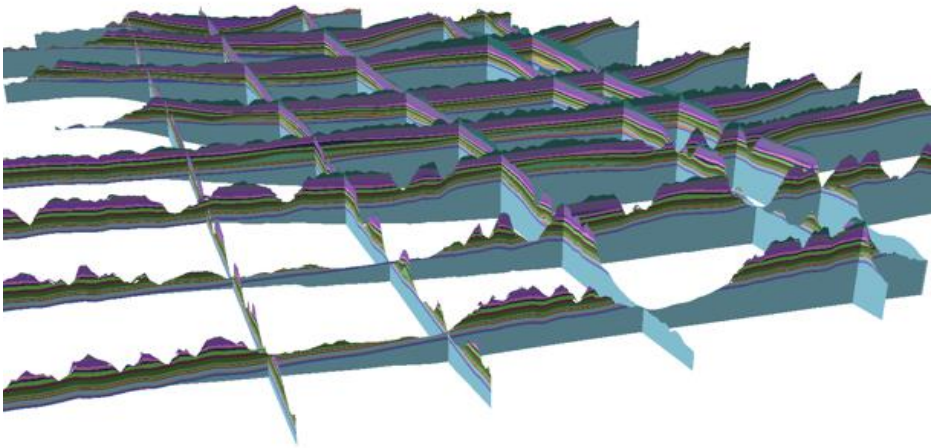

Figure 6. A fence diagram in ArcGIS stored in a 3D dataset in the project database exported from the 3D geologic framework.

As part of the 3D geologic framework output and input file generation for the system dynamic model an initial retort-distribution grid was created to generate individual retort cells for detailed data interpolation (Figure 7). Each grid cell can be input into the 3D geologic framework to create a retort block (Figure 8). Other datasets can then be interpolated into the 3D retort framework including fisher assay resource assessments, water content, fracture distribution and hydrogeologic parameters (Figure 9). The intention of the generating the individual retort cells was to produce data input files for the system dynamic model. This assists specific spatial locations for estimating water usage with time that needed to process each retort column within the model.

Zhou, W., Minnick M. D., and Cui, C. (2018) GIS for Natural Resources (Mineral, Energy, and Water). In: Huang, B. (Ed.), Comprehensive Geographic Information Systems Vol. 2, pp. 158–186. Oxford: Elsevier. ISBN: 9780128046609 https://doi.org/10.1016/B978-0-12-409548-9.09643-3

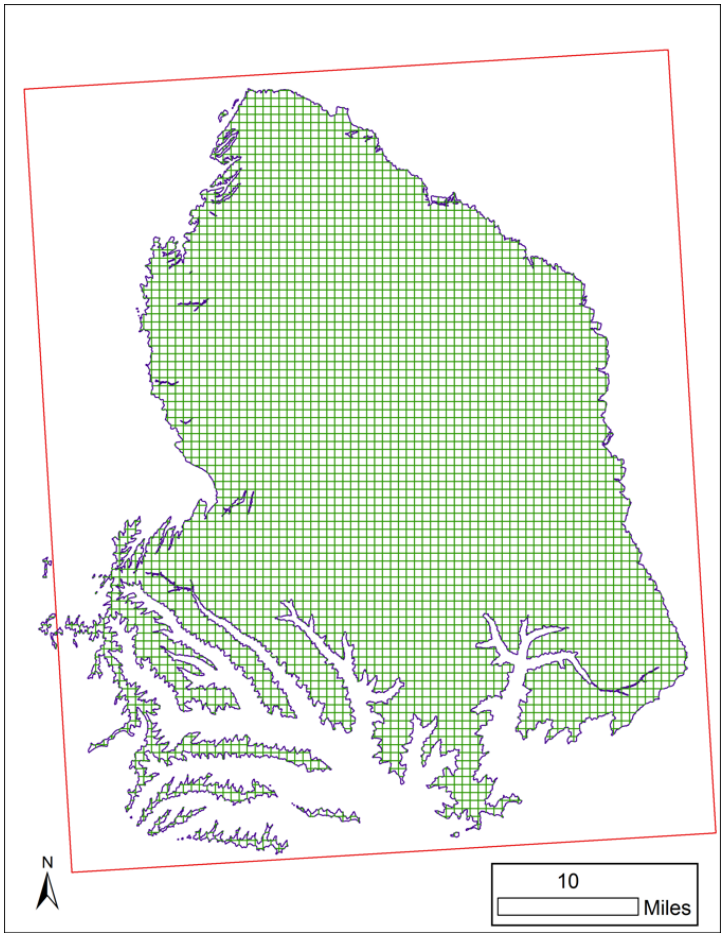

Figure 7. Map of initial grid used to generate spatially tied retort cells within the 3D geologic framework.

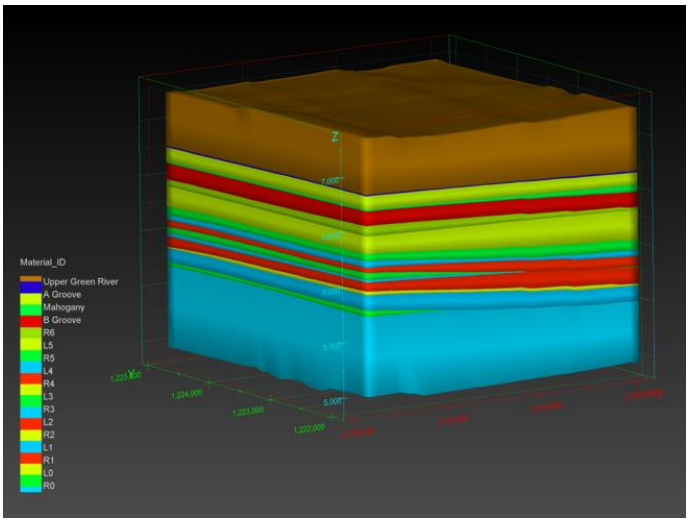

Figure 8. Single retort cell or column within the Green River Formation. The dimensions of a cell are 3000 x 3000 x 2300 ft.

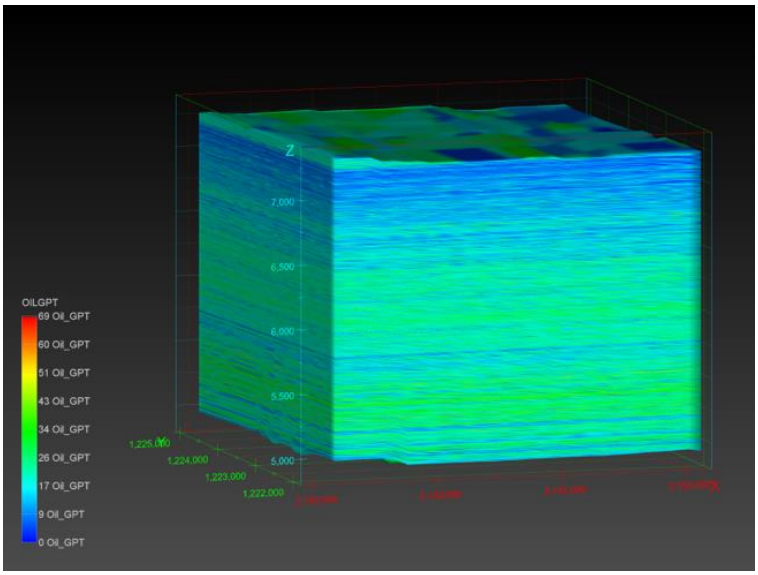

Figure 9. Image of a cell which displays Fischer Assay data, oil shale resource gallons/ton, interpolated into extracted retort framework.

2.3.2 Three-Phase Energy Resource Development Systems Models

In order to evaluate the water balance for *in-situ* oil shale conversion, a system dynamic model was construction (Mattson et al., 2012) using the Powersim Studio 9™ (version 9.01) software package. Three phases of an *in-situ* retort were considered: (1) a construction phase primarily accounts for water needed for drilling and water produced during dewatering, (2) an operation phase includes the production of water from the retorting process, and (3) a remediation phase involves water to remove heat and solutes from the subsurface as well as return the ground surface to its natural state (Mattson, et al., 2012). Throughout these three phases, the water is consumed and produced. Consumption of water is account for through the drill process, dust control, returning the ground water to its initial level and make up water losses during the remedial flushing of the retort zone. Production of water is through the dewatering of the retort zone, and during chemical pyrolysis reaction of the kerogen conversion. The major water consumption was during the remediation of the *in-situ* retorting zone (Mattson et al., 2012).

A large-scale hypothetical *in-situ* oil shale retort was simulated with the Powersim system dynamic model in the Piceance Basin. The Shell experimental area is in the northwestern part of the Piceance Basin, and the retorting site location was southwest of the Shell demonstration sites #1 and #3 as shown in Figure 10 and was assumed to have a dimension of 3000 by 3000 feet. At this location, subsurface information from well CO213 was assessable in the geodatabase (see Table 2). Based on this information it was assumed that oil shale from the A-Groove through the L-0 unit would be retorted. The total volume of the retort is about 360 million cubic meters.

Zhou, W., Minnick M. D., and Cui, C. (2018) GIS for Natural Resources (Mineral, Energy, and Water). In: Huang, B. (Ed.), Comprehensive Geographic Information Systems Vol. 2, pp. 158–186. Oxford: Elsevier. ISBN: 9780128046609 https://doi.org/10.1016/B978-0-12-409548-9.09643-3

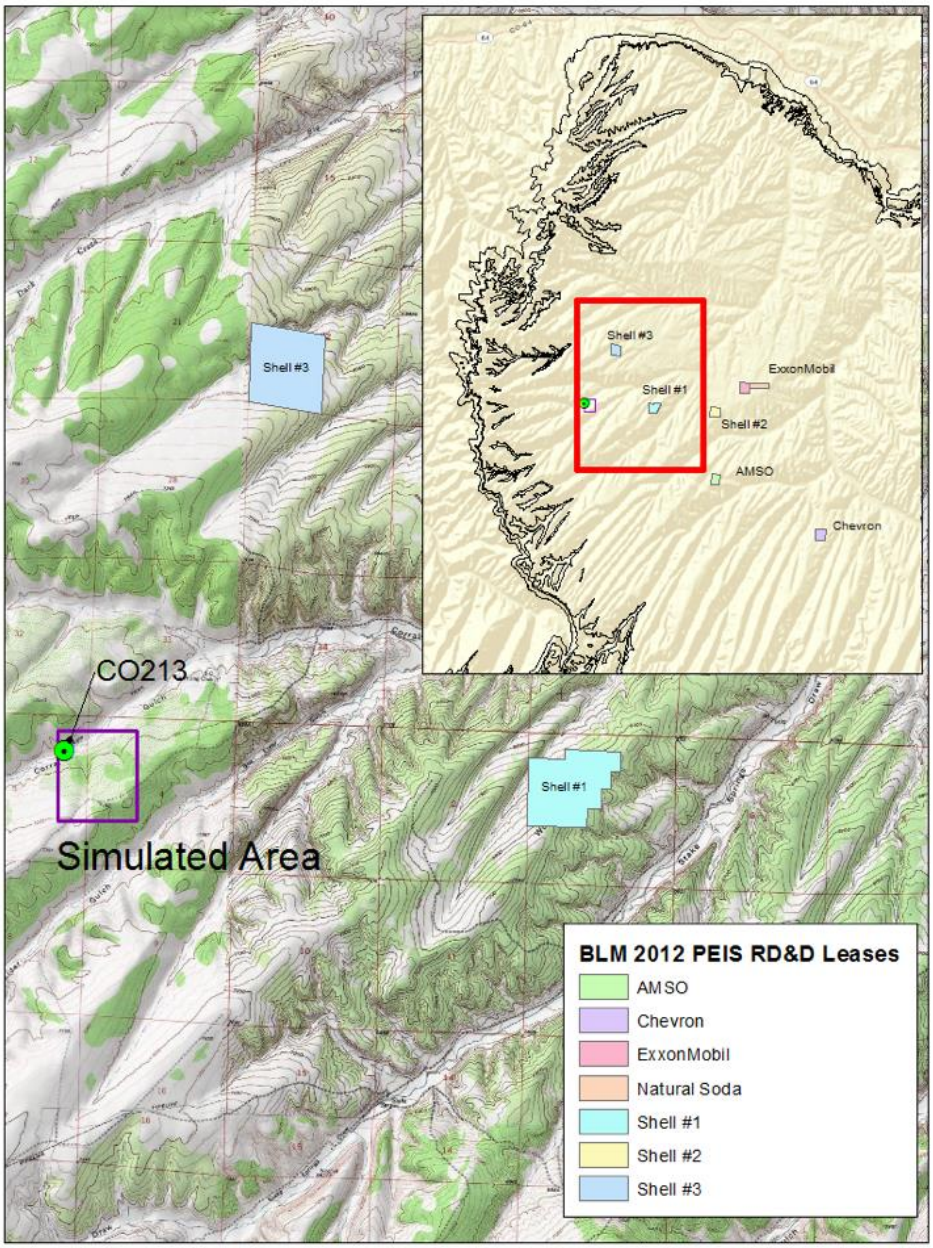

Figure 10. The simulated retort location is in the northwestern part of the Piceance Basin.

Zhou, W., Minnick M. D., and Cui, C. (2018) GIS for Natural Resources (Mineral, Energy, and Water). In: Huang, B. (Ed.), Comprehensive Geographic Information Systems Vol. 2, pp. 158–186. Oxford: Elsevier. ISBN: 9780128046609 https://doi.org/10.1016/B978-0-12-409548-9.09643-3

Table 2. Subsurface information of a retorting cell obtained from the integrated geodatabase (Zhou et al., 2015).

Layer name	Average thickness (m)	Volume (10^6 m^3)	Porosity (%)	Hydraulic conductivity (cm/day)	Average oil (GPT) based on CO213	Water in matrix (PGT)	Oil volume (gal)
Upper GRF	121.3	101.4	10	36.6	N/A	N/A	
A Groove	3.7	3.2	10	36.6	6.2	1.3	44,104,320
Mahogany	36.3	30.6	1	0.3	25.4	3.8	1,711,756,800
B Groove	7.3	6.1	10	36.6	5.7	1.0	76,826,880
R6	36.0	30.3	1	0.3	19.9	3.4	1,328,683,200
L5	24.7	20.9	10	18.3	11.7	5.4	538,068,960
R5	55.2	46.4	15	12.2	28.9	9.0	2,957,510,400
L4	20.1	16.8	20	61.0	21.8	7.1	806,669,760
R4	21.3	18.0	15	12.2	33.3	4.8	1,321,557,120
L3	11.3	10.8	8	12.2	11.3	4.5	27,006,0960
R3	22.9	19.2	1	0.3	24.5	4.2	103,958,4000
L2	7.9	7.1	5	6.1	15.3	4.8	237,725,280
R2	24.4	20.4	1	0.3	26.9	6.4	1,211,920,320
L1	9.4	8.0	3	6.1	5.4	10.5	9,4685,760
R1	33.8	28.3	0.5	0.3	19.4	9.1	1,210,560,000
L0	14.3	12.0	3	6.1	5.5	7.8	145,860,000
R0	43.9	36.8	0.5	0.3	N/A	N/A	

The models of the three phases were run independently from one another and therefore water production/consumption of the three phases must be sequentially added. Figure 11 illustrates the cumulative water consumption for all phases of the hypothetical retort. Positive slopes represent water production while negative slopes represent water consumption. As shown in Figure 11, although some water is consumed during drilling and dust control, water is generally produced in the first half of a retort operation due to dewatering of the retort volume and steam production of residual water during heating, whereas water is consumed in the final remediation phase.

Overall, approximately 500 million barrels (~15.75 billion gallons) of water is consumed (loss) for this hypothetical retort (Figure 11). However, the retort is calculated to produce 341 million barrels of oil. The ratio of water to oil is 1.47 and is in the range of what the industry has claimed as the expected water use rate. Data generated by the in situ retort system dynamic model can be imported into the geodatabase for subsequent analysis of the available water resources within the basin.

Zhou, W., Minnick M. D., and Cui, C. (2018) GIS for Natural Resources (Mineral, Energy, and Water). In: Huang, B. (Ed.), Comprehensive Geographic Information Systems Vol. 2, pp. 158–186. Oxford: Elsevier. ISBN: 9780128046609 https://doi.org/10.1016/B978-0-12-409548-9.09643-3

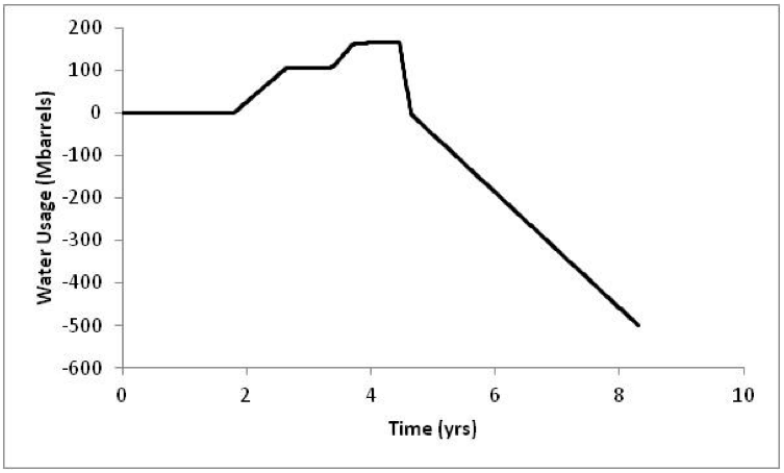

Figure 11. Cumulative water extracted verses temperature from hypothetical simulation. Water production is shown as positive water usage value, while water consumption is shown as negative water usage value.

2.4 Summary

A GIS-based water resource geospatial infrastructure in supporting of oil shale development has been developed in this project. The geospatial infrastructure not only serves as a repository for managing large volumes of geological, hydro-geological, topological, water resource and oil shale data but also as the groundwork for generating input data for different analytical models. The geodatabase within the geospatial infrastructure allows for collaborative regional/basin-wide assessments for future oil shale development based on the same "baseline". This type of collaboration provides an ideal atmosphere for the development of new, generically approaches that utilize new technology, and procedures that promote the best and most widespread use of our enormous data holdings despite their disparate locations and heterogeneous formats.

The components of this geospatial infrastructure were designed to be interlinked. These components include data frame, geodatabases, as well as customized tools and analytical models. The interlink allows for "synchronized" updating. The final results of this project support decision makers to make informed decisions. The procedures/tools/models developed in this research were designed to be general. These procedures/tools/models are readily adaptable to other similar study areas.

3.0 GIS Application in Assessment of the Vulnerability of Surficial Aquifer System for the State of Florida, USA

3.1 Background

There are three main aquifer systems in the State of Florida, namely the Surficial Aquifer System (SAS), the Intermediate Aquifer System (IAS), and the Floridian Aquifer

System (FAS) (Figure 12). While the IAS and the FAS are mostly confined, the SAS is comprised of unconfined aquifers, including the Sand and Gravel Aquifer and the Biscayne Aquifer. Due to its proximity and connectedness to the land surface, the SAS is highly susceptible to direct infiltration of contaminants from Onsite Wastewater Treatment Systems (OWTS) (Arthur et al., 2007). This study only focuses on the vulnerability of the SAS due to OWTS.

In the State of Florida, OWTS has been a feasible and economical wastewater treatment option for about 30% of Florida's population (Florida Department of Health, 2014). OWTS release nitrogen rich effluent mostly in the form of ammonium and nitrate, negatively impacting human and environmental health. Groundwater contamination from OWTS may reach the SAS and surface water bodies via percolation and subsurface transport of nitrogen. The detrimental impact of excess nitrogen in the environment warrants vulnerability studies that allow the delineation of areas more or less susceptible to contamination from land use practices (Cui et al., 2016).

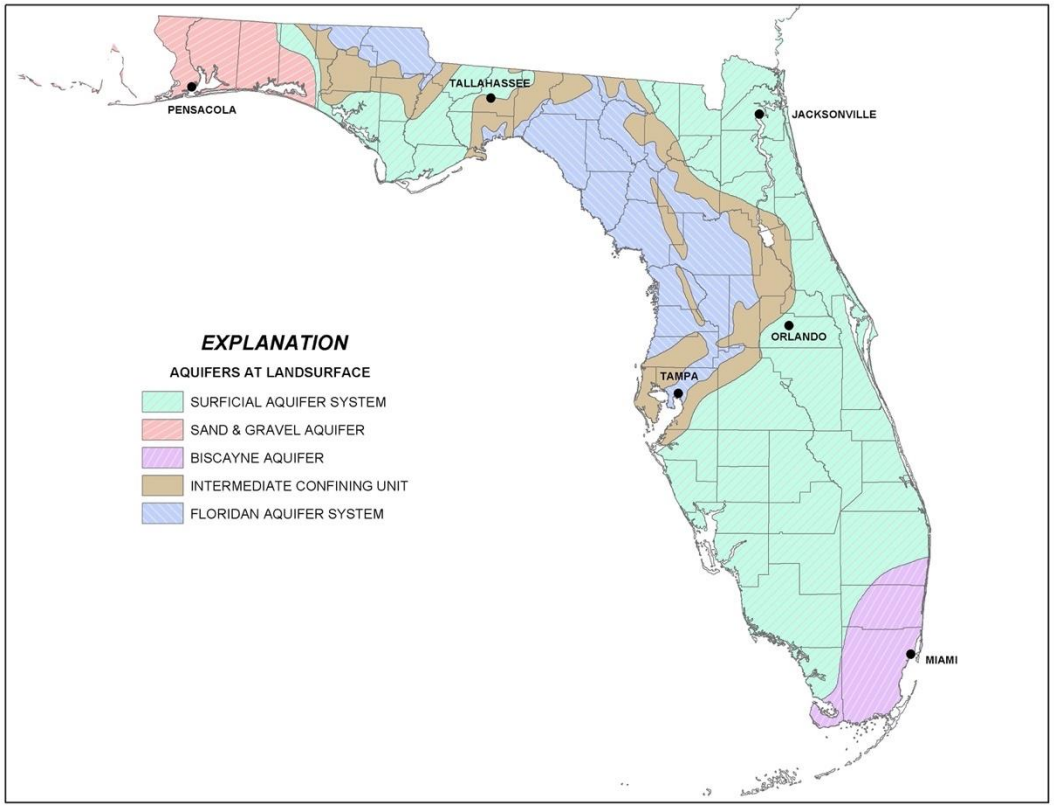

Figure 12. Map of aquifer systems and their extent in the State of Florida (Florida Department of Environmental Protection, undated).

A regional-scale GIS-based nitrogen fate and transport model (GIS-N model) was developed to assess aquifer vulnerability to contamination by examining the fate and transport of ammonium and nitrate from OWTS. The GIS-N model analyzed fate and

transport of nitrogen through the unsaturated zone using a simplified advection-dispersion equation (ADE) incorporated into a GIS framework. Operational inputs considered in this model include wastewater effluent ammonium or nitrate concentration and hydraulic loading rates. The GIS-N model considers two different approaches: single-step and two-step modeling approaches. The single-step model considers a denitrification process assuming all the ammonium is converted to nitrate before land application, while the two-step model uses ammonium as an input and considers nitrification followed by denitrification. The two approaches were evaluated for two nitrogen application scenarios: a uniform blanket input of nitrogen to the entire study area and a spatially variable input based on existing OWTS locations. The resulting maps from the different modeling approaches were classified into vulnerability zones based on the natural breaks in the data histogram. It was revealed that ground water vulnerability from OWTS is sensitive to the depth to water table and first-order reaction rates, as well as parameters controlling the time and amount of conversion respectively. Nitrate concentration is highest in areas with shallow water table depth. The vulnerability maps produced in this study will facilitate planners in making informed decisions on placement of OWTS and on groundwater protection and management (Cui, 2014).

In the following sections, the study of GIS application in assessment of the vulnerability of SAS for the State of Florida will be presented. This is a synthesis of previously published or non-published works by a research group at the Colorado School of Mines (Cui, 2014; Cui et al., 2016). The presentation of this project will be started with data collection, followed by methods, input parameters, GIS implementation of the models, results, and ended with summary.

3.2 Data Collection

GIS data for this study were acquired from various sources, including the Natural Resources Conservation Service (NRCS) soil survey, Florida Department of Environmental Protection, Florida Department of Health, Florida Fish and Wildlife Conservation Commission, and Florida Geographic Data Library (FGDL). Table 3 summarizes data sources of parameter values and spatial data used in the study. The NRCS provides soil data for the entire State of Florida from the Gridded Soil Survey Geographic (gSSURGO) database in the format of an Environmental Systems Research Institute, Inc. (ESRI) file geodatabase. Attributes used from the NRCS database include soil organic carbon, soil water content at field capacity, density, soil temperature, and soil texture. Locations of OWTS, effluent concentration, and loading rates were obtained from the Florida Department of Health. Florida land cover data were obtained through the Florida Fish and Wildlife Conservation Commission. Other parameters used in the contaminant removal calculation were obtained from literature and reports. Nitrification, denitrification and sorption rates were obtained from peer reviewed literature.

Zhou, W., Minnick M. D., and Cui, C. (2018) GIS for Natural Resources (Mineral, Energy, and Water). In: Huang, B. (Ed.), Comprehensive Geographic Information Systems Vol. 2, pp. 158–186. Oxford: Elsevier. ISBN: 9780128046609 https://doi.org/10.1016/B978-0-12-409548-9.09643-3

Table 3. Summary of datasets and sources

Name	Source	Description	GeoDatabase Feature
Gridded Soil Survey Geographic database	U.S. Department of Agriculture (USDA)	Soil data displayed as tables and maps	GeoRaster and tables
Wastewater inventory database	Florida Department of Health	Active OWTS locations	Polygon feature class
Porosity	Rawls et al., 1982	Porosity values for USDA soil textures	GeoRaster
Coefficients	STUMOD McCray et al., 2005	Values for coefficients used in equations	GeoRaster
Temperature Regime	Water Environment Research Foundation from USDA	Soil temperature regime	GeoRaster
FL land cover	Florida Fish and Wildlife Conservation Commission	Water bodies and wetland	Polygon feature class

3.3 Methods for SAS Vulnerability Assessment

The contaminant fate and transport approach was used in determining aquifer vulnerability. The spatial variability of the input parameters was taken into account by implementing the approach on a GIS platform.

3.3.1 Transport Equation

The calculation for contaminant removal in the vadose zone was based on the simplified advection-dispersion equation in N-CALC (Rao et al., 1985; McCray et al., 2010). The contaminant removal equation accounts for contaminant removal through first-order nitrification and denitrification processes and considers operational parameters (effluent concentration, effluent loading rates, porosity, and soil depth) and sorption and reaction parameters for nutrient transformation (linear sorption, nitrification rates, and denitrification rates) (Jury et al., 1987; McCray et al., 2010). The simplification ignores the effects of dispersion and assumes steady state conditions (Schlosser et al., 2002).

The simplified contaminant removal equation is an exponential decay function, which calculates the concentration of ammonium and nitrate as a function of the removal processes, expressed as:

$$C(Z) = C_0 exp\left(\frac{-RK_r}{v_z} Z\right) \qquad (1a)$$

$$C(Z) = exp(-RK_r.T) \qquad (1b)$$

where C_o is the initial concentration of ammonium or nitrate (mg L^{-1}), Z is the soil depth (cm), v_z is the vertical water velocity evaluated as hydraulic loading rate divided by porosity (cm day^{-1}), K_r is the first-order reaction rate (nitrification for NH_4^+ and denitrification for NO_3^-), and R is the retardation factor. The equation includes reaction rates, retardation, applied effluent concentration and the travel time for attenuation of contaminants. Note that Z/v_z in equation (1a) was replaced by travel time (T) in equation 1b. The velocity was estimated as hydraulic loading rate divided by the porosity assuming at steady state (Cui et al., 2016).

3.3.2 Fate Component: effects of environmental factors on N transformation

Nitrogen transformation is microbially facilitated and thus, affected by environmental factors that influence soil microbial activity. The GIS-N model considers the effect of environmental factors on biological reaction rates by adjusting the maximum reaction rate occurring at optimum environmental conditions for the effect of soil temperature and soil moisture. Those factors, defined as response functions, are combined linearly and reflect the non-optimum conditions controlling the first-order biological reaction rates.

The first-order reaction rate, K_r, is defined as the maximum reaction rate after adjustment for non-optimal biological activity. K_{rmax} is adjusted for the effect of soil temperature, soil moisture, and soil organic carbon content. The effect of those processes on the first-order reaction rate is represented by response functions which are empirical factors accounting for non-optimal conditions, expressed as:

$$K_r = K_{rmax} f_t f_{sw} f_z \qquad (2)$$

where K_{rmax} is the maximum first-order reaction rate (day^{-1}), f_t is soil temperature response function, f_{sw} is the soil moisture response function, and f_z is the soil organic carbon response function.

Soil temperature regulates organic carbon decomposition and nitrogen transformation processes. The temperature response function accounts for the influence of increase or decrease in temperature deviation from the optimum biological process rate, with a maximum value at optimum temperature (Youssef, 2003). The temperature response function used for both nitrification and denitrification is based on the Van't Hoff equation:

$$f_t = exp\left[-0.5\beta T_{opt} + \beta T\left(1 - \frac{0.5T}{T_{opt}}\right)\right] \qquad (3)$$

where T is soil temperature (°C), t_{opt} is the optimum temperature (°C) at which f_t equals unity, and β is an empirical coefficient (Youssef, 2003). The Van't Hoff equation describes the temperature effect on the nitrification and denitrification processes and accounts for the temperature sensitivity. The temperature response function results in

values between 0 and 1, with the value of 1 at the optimum temperature and less than 1 at soil temperatures below and above the optimum (Youssef, 2003).

Soil moisture content is another sensitive parameter in the nitrification and denitrification processes. Nitrification rates significantly decrease when soil moisture content exceeds an optimum amount and may cease at saturation. On the other hand, denitrification conditions are optimal as the relative soil moisture content reaches its maximum at complete saturation (Youssef, 2003; Barton et al., 1999). The response function for soil moisture is based on relative saturation rates at field capacity. The soil moisture response for denitrification, f_{sw} is expressed as:

$$f_{sw,dn} = \begin{cases} 0 & s < s_{dn} \\ \left(\dfrac{s - s_{dn}}{1 - s_{dn}}\right)^{e1} & s \geq s_{dn} \end{cases} \tag{4}$$

where s is the relative saturation, s_{dn} is a threshold relative saturation below which denitrification does not occur, and e_1 is an empirical exponent. S is the relative saturation as the ratio of actual moisture content to moisture content at saturation ranging from 0 to 1. Because of the lack of actual moisture data, the field capacity was used in place of the soil moisture content.

The soil moisture response function for nitrification is expressed as:

$$f_{sw} = \begin{cases} f_s + (1 - f_s)\left(\dfrac{1 - s}{1 - s_h}\right)^{e2} & s_h < s \leq 1 \\ 1 & s_l \leq s \leq s_h \\ f_{wp} + (1 - f_{wp})\left(\dfrac{s - s_{wp}}{s_l - s_{wp}}\right)^{e2} & s_{wp} \leq s < s_l \end{cases} \tag{5}$$

where s is the relative saturation (field capacity), s_h and s_l are the upper and lower limits of the relative saturation range within which nitrification proceeds at optimum rate, s_{wp} is the relative saturation at permanent wilting point, f_s and f_{wp} are the values of the soil water function at saturation and permanent wilting point, respectively, and e_2 is an empirical exponent (McCray, et al., 2010; Youssef, 2003).

The last function controlling the first-order rate process equation is the organic carbon response function, f_z. In denitrification, microbes use soil organic carbon as an electron donor to obtain energy through oxidation (Rivett et al., 2008). The organic carbon content in soil varies with depth. The rate adjustment factor for the organic carbon response function (f_z) is 1 when organic carbon is not limiting. In this study, organic carbon is assumed as non-limiting due to organic matter continuously supplied from the applied wastewater effluent (McCray et al., 2010). Furthermore, for nitrification, carbon

dioxide gas is the main energy source for the microorganisms. Soil gas is known to have high concentrations of CO_2 (Jury and Horton, 2004) thus, it is assumed that sufficient carbon will always be present for nitrification, providing that gas diffusion was not inhibited due to high soil water contents.

An additional process of retardation, represented by R in equation (6) is considered for the positively charged ammonium adsorbing to negatively charged soils. On the other hand, nitrate is considered to not sorb and thus, has a retardation factor of 1. Retardation is defined as:

$$R = 1 + \frac{K_d}{\theta}\rho \qquad (6)$$

where ρ (g cm^{-3}) is the bulk density of the soil, K_d (L kg^{-1}) is the distribution coefficient, and θ (%) is the soil moisture content. K_d, the distribution coefficient, is dependent on soil types and independent on water content (McCray et al., 2005).

3.4 Model Input Parameters

The model input parameters that describe the nitrification and denitrification processes include the first-order reaction rate, sorption, and operational parameters. The operational parameters considered in this nitrogen removal model include effluent concentration, hydraulic loading rates, porosity, depth to water table, soil moisture, and soil temperature. The following sections will provide a brief description of each of these parameters. Please refer to Cui (2014) and Cui et al. (2016) for detailed information on how the values of these parameters were determined.

Onsite wastewater treatment system effluent releases organic nitrogen that is readily decomposed into ammonium. The total nitrogen concentration in conventional OWTS effluent is assumed to be in the form of ammonium-nitrogen with a median concentration of 58 mg L^{-1}, thus a value of 60 mg L^{-1} NH_4^+ nitrogen is used as the ammonium input concentration for the nitrification process in the single-step and two-step models (McCray et al., 2005).

The Florida Department of Health maintains a statewide inventory of onsite sewage treatment and disposal systems for the State of Florida. The 2009 wastewater inventory database was used in this study. For parcels with an unknown wastewater treatment method, a logistic regression model was used to estimate the probability of the parcel being on an active OWTS based on parcels with a known wastewater treatment method (EarthSTEPS, LLC and GlobalMinda, 2009).

While nitrates do not readily sorb onto soil, ammonium exhibits sorption, which slows the transport of the contaminant and allows its transformation to nitrate via nitrification. Sorption is an important process controlling ammonium transformation. Ammonium is adsorbed during the wetting pulse of effluent application and is held onto the soil for nitrification when the soil dries (Ramesh Reddy and Delaune, 2008). The

cation exchange process of the ammonium sorption process is assumed to be linear, in equilibrium, and reversible (McCray et al., 2010).

The seepage velocity is dependent on the effluent hydraulic loading rate and the porosity for corresponding USDA soil textures. A hydraulic loading rate (HLR) of 2 cm day^{-1} for subsurface trenches was used as a representative value for drain field discharge (McCray et al., 2010). The porosity values from Rawls et al. (1982) were used for the seepage velocity calculation and correspond to the USDA soil textures (Table 4). Soil texture refers to the relative proportion of particles of various sizes in a given soil and affects the percolation rate of a soil. Coarser soil textures retain less water than fine grain soils, allowing the contaminated water to leach into the subsurface faster (Witheetrirong et al., 2011).

Table 4. Porosity classified by soil texture (Rawls et al., 1982)

USDA Soil Texture	Sample Size	Total Porosity/Saturation, Θ_s (cm^3/cm^3)
Sand	762	0.437
Loamy sand	338	0.437
Sandy loam	666	0.453
Loam	383	0.463
Silt loam	1206	0.501
Sandy clay loam	498	0.398
Clay loam	366	0.464
Silty clay loam	689	0.471
Sandy clay	45	0.430
Silty clay	127	0.479
Clay	291	0.475

The depth to water table controls the depth available for contaminant transformation from microbial activity in the vadose zone as described by the travel time (Z/v_z) in equation (1a). The USDA annual minimum water table depth field for soil depth input is measured as the shallowest depth to a wet soil layer (water table) at any time during the year expressed in centimeters from the soil surface, for components whose composition in the map unit is equal to or exceeds 15%. The depth to water table layer using the recorded representative value with a range of 0 to 203 cm.

The maximum reaction rate (K_{rmax}) is adjusted by factors calculated as response functions: f_t, f_s, and f_z to represent non-optimal conditions. The first-order maximum nitrification and denitrification rate coefficients were obtained from the cumulative frequency diagram (CFD) of reaction rates developed by McCray et al. (2005) (Figure

13). The CFDs were created based on literature review of nitrification and denitrification rates observed for natural soils under both saturated and unsaturated conditions (Heatwole and McCray, 2007; Anderson and Otis, 2000).

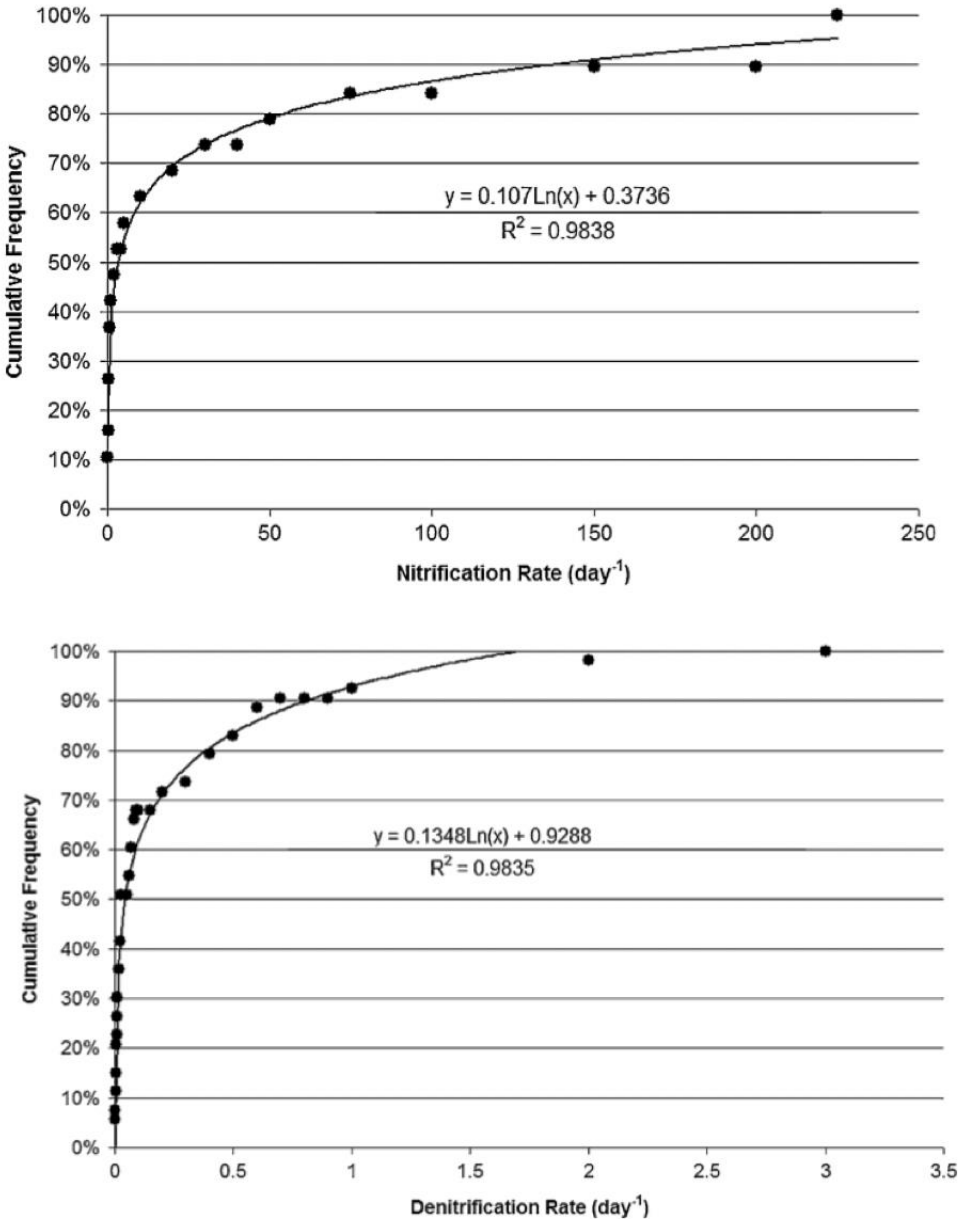

Figure 13. CFD for the first-order nitrification rate and denitrification rate (McCray et al., 2005).

The nitrogen transformation rate increases with increasing soil temperature until the optimal value of 25°C and declines with additional increases in temperature (McCray et al., 2010). The temperature function for both nitrification and denitrification is represented by equation (3). The soil temperature (T) for Florida is determined from the

USDA soil annual average temperature map for the contiguous United States. The USDA assigns soil temperatures based on the interpolation between Natural Resources Conservation Service (NRCS) soil temperature stations or through extrapolation.

The soil organic carbon content is assumed to be non-limiting for the nitrogen transformation process due to the introduction of organic carbon with OWTS effluent. The soil organic carbon response function is set to 1 to represent the presents of sufficient carbon.

Soil moisture content affects the diffusivity of gases into the soil, controlling oxygen availability to nitrify microbes. The soil moisture function for nitrification represents the optimal relationship between substrate and available oxygen levels (McCray et al., 2010). The soil moisture function for the transformation processes is represented by equations (4) and (5). The relative saturation is calculated as the soil moisture at field capacity divided by porosity. Field capacity was used as the soil moisture value due to limited soil moisture data. Additional parameter values for coefficients present in the equation are listed in Table 5. The soil moisture function values for the nitrification and denitrification reaction rate adjustment calculation were performed in GIS.

Table 5. Coefficient values used for soil moisture function

Parameter	Value
S_{dn}	0
e	1.4
e_1	1
e_2	1
S_h	0.85
S_l	0.5
s_{wp}	0
F_s	0
F_{wp}	0

The first-order reaction rate (K_r) for the nitrification and denitrification process is the maximum reaction rate adjusted by the response functions for non-optimal biological activity. The combination of the maximum reaction rate, soil temperature function, soil moisture function, and the soil organic carbon content function is represented by the K_r values. The first-order reaction rate after adjustment for the nitrification and denitrification reaction ranges from $3.25 – 0.36 day^{-1}$ to $0.27 – 0.0046\ day^{-1}$, respectively, with a K_{rmax} value at $3.25\ day^{-1}$ and $0.27\ day^{-1}$, respectively.

3.5 GIS Model and Implementation

The Florida aquifer vulnerability model was implemented in a GIS platform. GIS allows the integration of spatial data in heterogeneous formats to represent spatially

variable events by relating a series of data layers (Bonham-Carter, 1996). In this study, ArcGIS 10.1 is used to process and manage spatial data through the input of created data layers. Each layer represents a variable in the contaminant removal equation and was algebraically combined based on the contaminant fate and transport equation. Performing the calculations in GIS allows the display of spatially variable data.

The spatially variable parameters used in the calculation were incorporated into the GIS-N model to produce zonation maps illustrating Florida's surficial aquifer vulnerability based on the concentration of ammonium and nitrate reaching the water table. The remaining concentrations maps were produced for four different modeled scenarios: single-step and two-step models with uniform blanket application, and existing OWTS application for both the single-step and two-step models.

3.5.1 Single-step process model with blanket application

The single-step GIS-N model simulates the nitrification and denitrification processes separately via a raster approach through the combination of layers based on the simplified advection-dispersion equations (1a) and (1b). Both processes were calculated with the depth to water table value set as the soil depth (Z) input. The remaining concentration output from the contaminant fate and transport equation was determined for the depth at the water table. For the single-step nitrification model, a uniform blanket application of 60 mg L^{-1} of NH4-N was applied to the entire State of Florida. The model utilizes the inputted concentration in the contaminant transport equation and produces results of remaining ammonium concentration. Similarly, the denitrification model utilizes the uniform input concentration of 60 mg L^{-1} of NO3-N to calculate remaining nitrate concentrations for a sensitivity analysis. The initial input concentration of 60 mg L^{-1} of NO3-N for the single-step denitrification model assumes all of the ammonium is converted to nitrate before application to the soil surface.

3.5.2 Two-step model with blanket application

The two-step GIS-N model calculates the nitrification and denitrification processes as dependent steps. The two-step model assumes the nitrification and denitrification processes occur in a stepwise manner and not simultaneously. The first step simulates the nitrification process with an input concentration of 60 mg L^{-1} of NH4-N with the soil depth equivalent to the depth to water table layer capped at a maximum of 31 cm, since at a depth of 31 cm below the soil treatment unit, the nitrification process is usually completed (Fischer, 1999; Beach, 2001). Any depth to water table distance remaining after 31 cm was used as the depth in the denitrification process. The input concentration for the denitrification process is the concentration of nitrate converted from the ammonium via the nitrification process in step one. Step two is the removal of nitrate through denitrification, providing final results of remaining nitrate concentration at the water table depth. For the blanket application approach, a uniform input concentration of contaminant is applied to the entire State.

3.5.3 Existing OWTS application for single-step and two-step models

The OWTS model calculates nitrogen removal with the single-step and two-step approaches based on effluent input at existing locations of active OWTS in a point feature approach. An initial concentration of contaminant was applied to the areas influenced by OWTS effluent discharge. Parameters from the developed raster layers were converted to point features classes for the calculation. The calculated result of remaining nitrate concentration from the single-step and two-step modeling methods provided information on areas currently affected by OWTS. The point feature results were then interpolated with the kriging method described below to provide a probability of nitrate exceeding a given threshold and areal extent of contaminant influence from OWTS effluent loading.

Kriging is a stochastic method for interpolation used to predict values for unmeasured locations by weighing the surrounding measured values based on autocorrelation. Kriging associates probability with the predictions and also assess the errors. Predictions are computed by assigning weights based on distance between measured points, prediction locations, and spatial arrangement among the measured points (ESRI, 2003). Points that are closer together are assumed to be more similar than points further apart. The observed trend which models autocorrelation as a function of distance can be described by different kriging models. Indicator kriging predicts the probability of a point exceeding a given threshold through the process of ordinary kriging.

Indicator kriging determines the probability of the remaining contaminant levels at the water table reaching the set threshold. The model is based on the equation described below:

$$I(s) = \mu + \varepsilon(s) \qquad (7)$$

where I(s) is a binary variable, μ is the unknown mean constant, and ε(s) is the autocorrelated error. Continuous data points are converted to binary values (0 or 1) based on the threshold, with 0 if the value is below the threshold and 1 if the value is above the threshold. The indicator kriging method was applied to the existing OWTS application for the single-step and two-step models. A different threshold was used for the single-step and two-step models based on the distribution of remaining nitrate concentration determined from the geometric interval.

3.6 Results

Florida surficial aquifer vulnerability maps were produced from the GIS-N single-step and two-step model with uniform blanket application, and existing OWTS application for the single-step and two-step models. The models indicated the likelihood of areas susceptible to nitrate contamination based on remaining nitrate concentrations

calculated from the contaminant fate and transport equation. Figure 14 shows the Florida surficial aquifer vulnerability map based on the two-step OWTS nitrogen removal model with vulnerability classification based on the natural break in the predicted probability of exceedance.

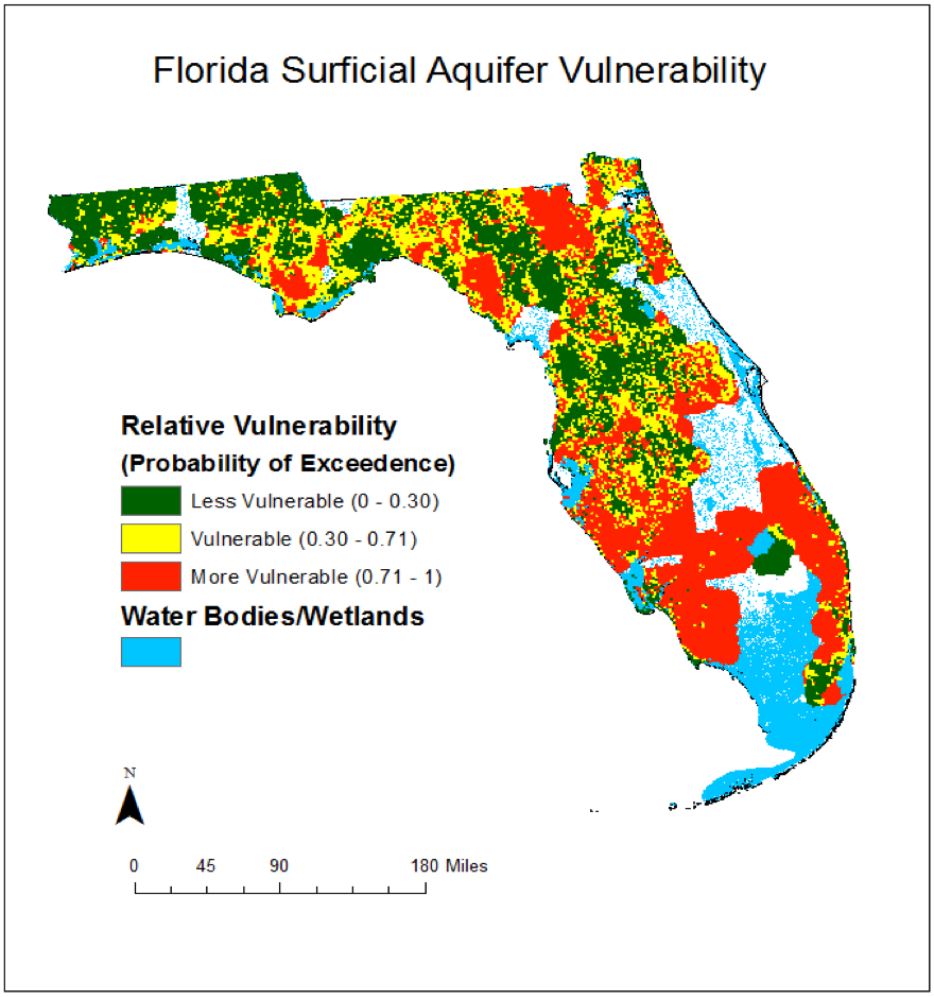

Figure 14. Florida surficial aquifer vulnerability map based on the two-step OWTS nitrogen removal model with vulnerability classification based on the natural break in the predicted probability of exceedance.

Among the four nitrogen removal models, each has different advantages and limitations. A comparison of the four models provided in Table 6 will assist in determining the optimal model to utilize in reducing the human and environmental impacts of land use decisions.

Zhou, W., Minnick M. D., and Cui, C. (2018) GIS for Natural Resources (Mineral, Energy, and Water). In: Huang, B. (Ed.), Comprehensive Geographic Information Systems Vol. 2, pp. 158–186. Oxford: Elsevier. ISBN: 9780128046609 https://doi.org/10.1016/B978-0-12-409548-9.09643-3

Table 6. Advantages and limitations of the different nitrogen removal models

Nitrogen Model	Advantages	Limitations
Single step- blanket application	• Provides sensitivity analysis • Most simple, with the least assumptions and uncertainty • Considers vulnerability based on soil conditions for the entire State	• Assumes 60 mg/L NO3 –N as initial contaminant concentration input • Not representative of current aquifer vulnerability conditions from OWTS effluent • Only considers the denitrification process
Two step- blanket application	• Calculates vulnerability based on soil conditions of the entire State • Considers both the nitrification and denitrification processes.	• Bias at shallow water table depth • Not representative of current aquifer vulnerability conditions • Nitrification and denitrification not modeled as simultaneous reactions
Single step- existing OWTS application	• Considers aquifer vulnerability from current location of OWTS	• Assumes 60 mg/L NO3 –N as initial contaminant concentration input • Estimate of vulnerability based on kriging interpolation not representative of radial extent of OWTS effluent • Only considers the denitrification process
Two step- existing OWTS application	• Considers aquifer vulnerability from existing OWTS effluent discharge • Considers both the nitrification and denitrification processes.	• Bias at shallow water table depth • Nitrification and denitrification not modeled as simultaneous reactions • Estimate of vulnerability based on kriging interpolation not representative of radial extent of OWTS effluent

3.7 Summary

Florida's surficial aquifer system (SAS) is vulnerable to contamination from anthropogenic sources stemming from land use practices. In Florida, onsite wastewater treatment systems (OWTS) contribute to nitrogen loading into the vadose zone and aquifer system. This study modeled the fate and transport of nitrogen in the vadose zone based on a simplified groundwater flow equation implemented in a GIS platform. The resulting aquifer vulnerability maps produced with spatially variable soil data will facilitate efforts of land management in protecting water resources for better human and environmental health. The key findings of the study are listed below:

1. Depth to water table in Florida is generally shallow, ranging from 0 cm to 203 cm with 24.3% the area ≤ 5cm. The most vulnerable areas correlate with shallow depth to water table measurements.
2. Zones within the Gravel and Sand Aquifer are less vulnerable. The lower vulnerability is attributed to the deeper depth to water table measurement. A lower vulnerability correlates with known occurrences of silt and clay confining lenses.

Zhou, W., Minnick M. D., and Cui, C. (2018) GIS for Natural Resources (Mineral, Energy, and Water). In: Huang, B. (Ed.), Comprehensive Geographic Information Systems Vol. 2, pp. 158–186. Oxford: Elsevier. ISBN: 9780128046609 https://doi.org/10.1016/B978-0-12-409548-9.09643-3

3. Streams near OWTS are of concern due to the discharge of the groundwater as baseflow. Groundwater from the SAS moves along quick and short flow paths, which can prevent any additional denitrification in the groundwater.

4.0 GIS Application in Analyzing the Offshore Placer Gold at Nome, Alaska, USA

4.1 Background

Nome is located on the southern coastline of the Seward Peninsula, on the northern coast of Norton Sound to the west of the State of Alaska (Figure 15). There is abundant Placer gold offshore (Koschmann and Bergendahl, 1968; Garnett, 2000) at Nome because fluvial and glacial processes transported gold from gold-enriched bedrock in the uplands into the marine environment where it was further concentrated by wave and current actions.

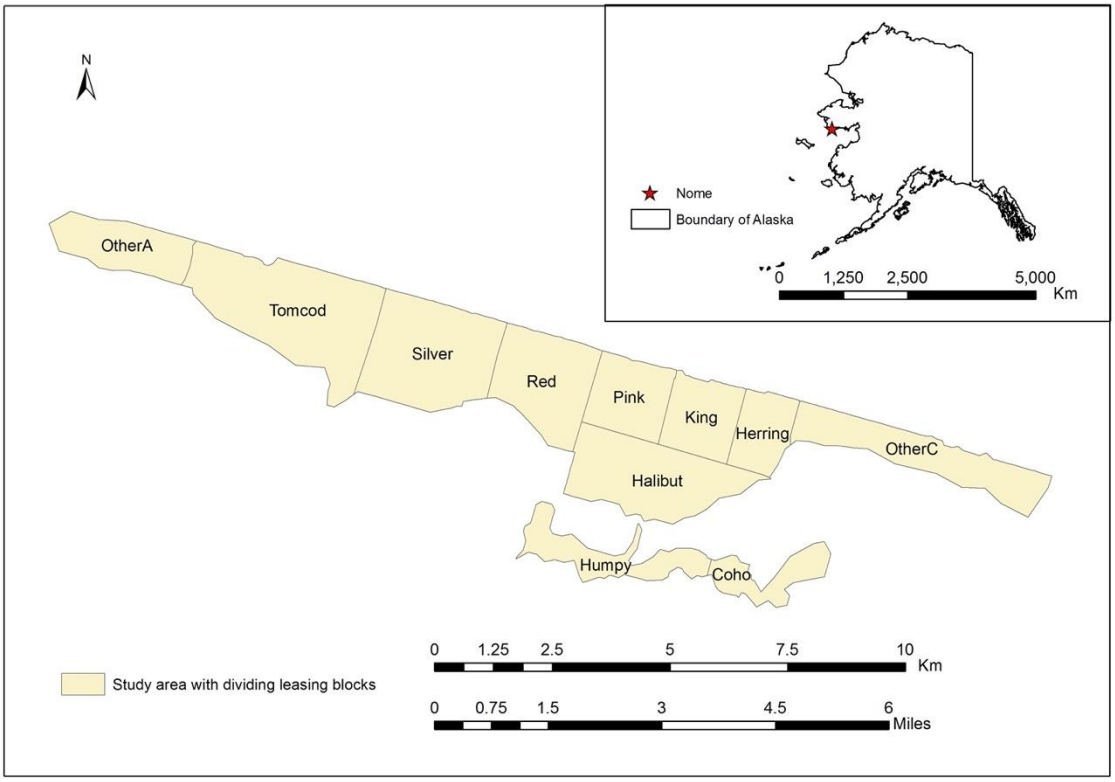

Figure 15. Location of the study site at Nome, Alaska. The individual block in the study site is for leasing purpose only. There are no geologic and bathymetric influences in dividing theses blocks.

The Nome offshore area was studied extensively due to the extent and richness of the placer gold resources. Geological, geophysical, and geochemical characteristics of offshore gold deposits were well documented in the literature. The USGS and United States Bureau of Mines (USBM) summarized much of the geology of the area (Nelson and Hopkins, 1972; Tagg and Greene, 1973; Bronston, 1990). There are 22

metasedimentary, metavolcanic, and metaplutonic bedrock units in the area. The Nome Group is a series of four lithostratigraphic units that are locally deformed by low-angle thrust faults. The Nome Group consists of the following four subunits (Bundtzen et al., 1994): (1) basal, complexly deformed quartz-rich politic schist, (2) mafic and pelitic schists and marble, (3) mafic-dominated schist assemblage, and (4) dirty marble (Bundtzen et al., 1994).

Nome is one of the most recently active areas of marine and beach placer mining in the State of Alaska (Koschmann and Bergendahl, 1968; Garnett, 2000). As early as 1897–1962, the Nome area produced about 5 million ounces of gold (Koschmann and Bergendahl, 1968). Because of the huge amount of data in variety of forms accumulated from placer gold exploration and production over the past century, the analysis and management of these data for future development of the Nome offshore gold resource is an enormous task. GIS technology is a tool well suited to meet this challenge. A GIS-based approach to data management provides an in-depth understanding of the Nome offshore gold deposit, which, in turn, will greatly assist the development of the offshore gold resource in that area.

In the following sections, a study of GIS application in placer gold resource estimation in Nome, Alaska will be presented. This is a synthesis of previously published or unpublished works by a research group at the University of Alaska Fairbanks (Huang et al., 2001; Chen et al., 2003; Chen et al., 2005; Li et al., 2005; Luo et al., 2005; Zhou et al. 2007; Zhou, 2009). The leading author of this chapter was part of that research team. The presentation of this case study will be started with data collection and geodatabase development, followed by methodology, resource estimation, and ended with summaries.

4.2 Data Collection and Geodatabase Development

Data sources for this study include private sectors of mining and mineral exploration, published literatures, unpublished reports, maps and open file reports from government agencies, documents from recording offices, and information through the Internet. During the summers of 1986 and 1987, WestGold Exploration Mining Company, Limited Partnership (WestGold) carried out 3400-line km of high-resolution seismic surveys of the lease area. Seismic data were interpreted to provide facies interfaces and thicknesses, allowing faulting to be identified and profiles to be drawn. Simultaneous side scan sonar surveys, with a 3-mm penetration, were used to map sediment type on the seafloor. From 1987 through 1989, WestGold completed 2530 holes and collected 57 bulk samples. Each hole was drilled in one-meter increments. The sediment from each one-meter interval was collected and stored, a brief sediment description was recorded and the gold content was assayed (Bronston, 1989).

Data files from 3468 drill holes in the offshore area at Nome were reformatted and complied. These file types were the principal sources of information for this project (Huang et al., 2001). Most drill hole logs record lithology, gold concentration value, and penetration blow count. Blow count data, the number of blows needed to drive each

barrel through a sample length of 30 cm, provides sediment hardness information. A geologic key describes lithologic types intercepted. Gold concentration values are tabulated in oz/m^3 and oz/yd^3, along with "reclassified" and "intensity" values. Reclassified value is the relative gold concentration as compared with a given reference. Intensity value shows reclassified gold values (from 0 to 45) as 9 even intervals with intensity of 9 signifying highest gold concentration.

The research team at UAF then re-compiled and integrated the information to study the geologic characteristics, geochemical and geophysical signatures, borehole data, economic considerations, oceanographic factors, submarine topography, and potential environmental impacts (Zhou et al. 2007; Zhou, 2009).

In this project, GIS was applied to analyze the offshore marine placer gold deposits at Nome, Alaska. Two geodatabases, namely Integrated Geodatabase (IG) and Regularized 2.5D Geodatabase (R2.5DG) were created in this study. The IG served as a data container to manage various geological data, such as borehole, bedrock geology, surficial geology, and geochemical data. The R2.5DG was generated based on the IG and was used for gold resource estimate. The two geodatabases are linked and related (cross-referenced) to each other through common attributes. Other features of this GIS infrastructure include data updating, query, analyzing, visualizing, and volume calculation. The gold resource estimation at various cutoff grades can be calculated interactively. A geostatistical study was carried out for optimizing the resource estimation approach. Figure 16 shows the flowchart of the conceptual GIS architecture of this project.

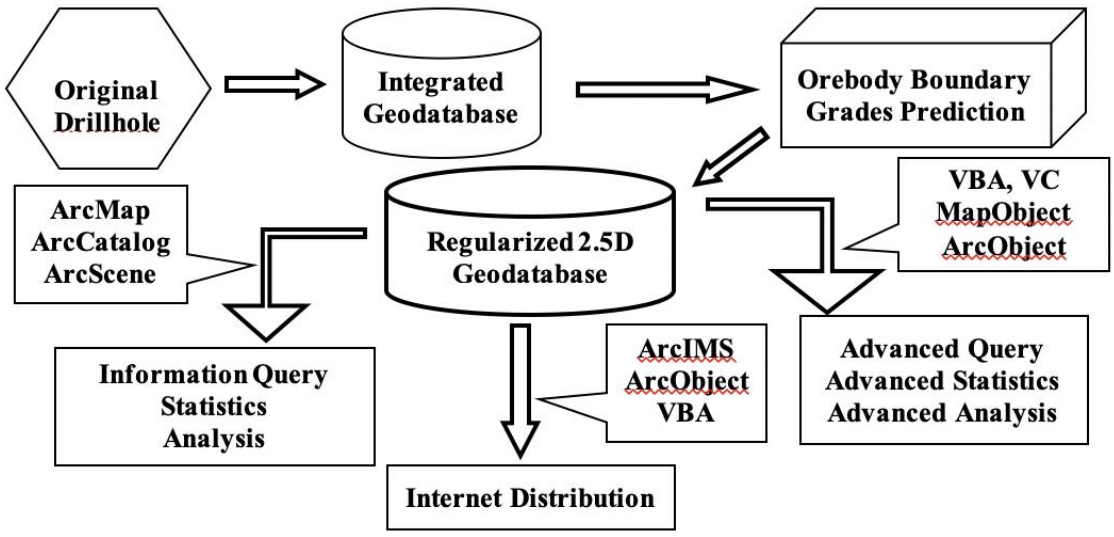

Figure 16. Conceptual GIS architecture of the project (Zhou et al., 2007)

Table 7 lists the feature classes stored in the IG. The IG is capable of displaying 3D surfaces using ArcGIS extensions, such as 3D Analyst, Geostatistics Analyst, and Spatial Analyst. However, it does not have the capability for solid three-dimensional

analyses and cannot yield information on volume calculation and resource estimation. In order to perform resource estimation, the Regularized 2.5-Dimensional Geodatabase (a quasi-3D geodatabase), was created by subdividing the study area into cells. The R2.5G is able to define ore body boundaries, perform grade extrapolation, and estimate the resource at any given spatial domain.

Table 7. List of Feature Classes in Integrated Geodatabase (Zhou et al., 2007)

Feature Class	Feature Type	Description
DH_location	Table	Drill hole location info
DH_segmentinfo	Table	Borehole segment attributes
DH_sliceinfo	Table	Layered orebody information
GeoDH_sliceinfo	Point	Layered orebody information
Lith_slice_Poly	Polygon	Layered lithology
OnshoreGeo	Polygon	Onshore geology
OffshoreGeo	Polygon	Ocean floor geology
Structure	Polygon	Offshore sediment structure elements
Permitblk	Polygon	Exploration permit blocks
Rivers	Polygon	Rivers, town and roads of Nome
Studyarea	Polygon	Study area boundary

The study area is approximately 40 km^2. There were 3468 drill holes distributed irregularly and spaced from 50 to 120 meters within the study area. The study area was divided into 10m by 10m grids to develop the regularized geodatabase. The division formed 404319 spatial records with one record for each cell. The finer the grid the more precise the result. However, finer grids would demand more computer storage and take longer time to perform ore resource estimation. For the purpose of this project, a 10m by 10 m grid is sufficient for the precision and yet time efficient to perform ore resource estimation (Zhou et al., 2007).

4.2 Methods for Offshore Placer Gold Resource Estimation

Any in-place resource calculation problems must deal with estimating two inter-related items: the grade and the associated volume. This grade could be the economic cut-off grade or the average grade within a pre-specified volume. The volume of ore can be estimated based on ore body boundary.

Five steps were used for in-place placer gold estimation. The first step for resource calculation is to determine ore body thickness and average gold grade for every borehole. Calculation of average gold grade for each borehole based on various cut-off grades is a time-consuming task. Since ore body boundaries are different at various cutoff grades, their

associated thickness and average grade also are different. The calculations are performed repetitively in MS Access using SQL language, based on segment records stored in the borehole segment information table in the Integrated Geodatabase. The calculated average grades and thicknesses of various layers form the layered ore body information table.

The second step is to create a point layer and grid coverage and add them in the 2.5D Geodatabase. The point layer is used to store the layered ore body grades and thicknesses. In this layer, the entire study area is divided into 10m×10m grids, and each point feature object in the center of a cell represents this cell and all of the grades and thickness are stored in this point object. The entire study area is approximately 40.4319 km^2. The Regularized 2.5D Geodatabase contains 404319 spatial point records, each point record representing one 10×10m-grid cell.

The third step is to determine the thickness for each cell created during the second step. The attribute data in GeoDH_sliceinfo layer is utilized to build ore body boundaries. To determine the ore body thickness of each regularized cell, two ore body boundaries are generated based on the levels of the ore body's beginning depth and the ending depth, respectively. The ore body boundaries are interpolated using the Natural Neighbor method, which is an interpolation method that estimates the value of a cell using weighted values of the input data points that are their natural neighbors, determined by creating a triangulation of the input points. The Natural Neighbor tool in ArcGIS can efficiently handle large numbers of input points. Other interpolators may have difficulty with large point datasets (ESRI, 2004b).

The next step is to interpolate the gold content for each regularized cell. Five interpolation methods are investigated and compared. IDW and IK were selected for interpolating the gold concentration contour maps (Li et al., 2005). The procedure of geostatistical analysis will be described in the next section.

The last step is to estimate the gold resource within the study area. After the thickness (T) and average grade (G) for each cell are obtained, one new column (G_ T) can be created to store $G_i \times T_i$. For any selected polygon area, $\sum(G_i \times T_i)$ and $\sum T_i$ can be obtained by using the "statistics" tool in ArcMap

The gold resource within a selected a polygon area is estimated by the following equation:

$$R = \sum(G_i \times T_i) \times 10 \times 10 \qquad (8)$$

where G_i is grade value of each cell above cutoff grade. T_i is thickness of each cell.

The average grade (G_{ave}) within a polygon area is given by:

$$G_{ave} = \frac{1}{\sum T_i} \sum (G_i \times T_i) \qquad (9)$$

Table 8 gives total resource estimates at different cutoff grades within the entire study area. Both the actual and normalized gold values are calculated and stored in the IG. Depending on the cutoff grade, the total amount of gold resource ranges from 113,767oz (with a cutoff grade of 1000 mg/m^3) to 2,309,664 oz (with a cutoff grade of 0 mg/m^3). The average grade ranges from 0.233 g/m3 (with a cutoff grade of 0 mg/m^3) to 1.929 g/m^3 (with a cutoff grade of 1000 mg/m^3).

Table 8. Resource estimations at different cutoff grades (Zhou et al., 2007)

Cut-off Grade (mg/m³)	Orebody Area (m²)	Average Thickness (m)	Average Grade (mg/ m³)	Ore Volume (m³)	Resource (Kg)	Resource (Oz)
0	40429800	7.63	0.233	308325290	71840	2309664
200	18060600	4.86	0.554	87737850	48607	1562718
500	2438900	5.28	1.047	12886388	13492	433772
800	740400	5.33	1.441	3948949	5690	182949
1000	404600	4.53	1.929	1834422	3539	113767

During the surface interpolation process, five geostatistical approaches that built-in in ArcGIS are evaluated and compared. These geostatistical approaches include Inverse Distance Weighted (IDW), Ordinary Kriging (OK), Ordinary Kriging with lognormal transformation (OK-log), Simple Kriging (SK) and Indicator Kriging (IK). Cross-validation is used to examine the accuracy of the five approaches. It is determined that the OK and SK algorithms are not suitable for this dataset because of the difficulty of fitting the semivariogram model despite their lower RMSE (Root-mean-square error) and the higher RMSS (Root-mean-square Standardized). The OK-log algorithm does not provide satisfactory prediction either, because it places too much weight on the role of extreme values resulting in overestimation and extremely high RMSE. Reserve estimation of each blocks is conducted using each of the interpolation methods and compared with the reserve calculated using the conventional polygon method. The IWD and IK algorithm seem to provide estimations more agreeable with the conventional polygon method. The geostatistical analysis will be briefly described next. Detailed information about this geostatistcial study can be found in Li et al. (2005).

IDW is one of the many methods to perform interpolation of scattered spatial data. A neighborhood about the point to be interpolated is selected and a weighted average is calculated of the observed values within this neighborhood. The weighting factors of observed points are a function of the distance between the observed points to the interpolated point, the closer the distance the bigger the weights. The interpolating function is constructed as a linear combination of the observed values v_i at point x multiplied with

weight functions w_i (Fisher et al., 1987):

$$f(x) = \sum_{i=1}^{n} v_i w_i(x) \qquad (10)$$

where the weight factors $w_i (i = 1,2...,n)$ are constructed by normalizing each inverse distance:

$$w_i(x) = d_i^{-\lambda_i}(x) \Big/ \sum_{j=1}^{n} d_j^{-\lambda_j}(x) \qquad (11)$$

where $d_i(x)$ is the Euclidean distance from point x to node x_i, and λ_i is the exponential power of weight. Each weight function w_i is inversely proportional to the distance from the point x_i where the value v_i is prescribed. The sum of the proportional factors $w_i (i = 1,2...,n)$ should equal to one.

The possible redundancy between samples depends not simply on the distance but also on the spatial continuity. Kriging methods, which use a customized statistical distance rather than a geometric distance to de-cluster the available sample data, are linear estimation that develops optimal weights to be applied to each sample in the vicinity of the block being estimated. They are based on the best linear unbiased estimation, which minimizes the mean error and the variance of the errors. They depend on the statistical model employed and the following mathematical formula.

$$Z(s) = \mu(s) + \varepsilon(s) \qquad (12)$$

where Z(s) is the value of interest, μ(s) is the deterministic trend and ε(s) is auto correlated errors.

The variable s indicates the location which is the spatial coordinates in ArcGIS. Based on different assumptions of the error term, ε(s), there are several different Kriging methods, such as Ordinary Kriging, Simple Kriging, Universal Kriging, Indicator Kriging, Cokriging and others. All of them are built-in in ArcGIS Geostatistical Analyst extension.

Cross validation is used for assessing the surface interpolation different Kriging methods. The Mean Standardized Prediction Errors (MSE) and the Root Mean Square Error (RMSE) are shown in Table 9.

The RMSE for estimates made using OK-log is the highest whereas for others they are almost the same. The OK-log algorithm will not provide satisfactory prediction either, because it places too much weight on the role of extreme values resulting in

overestimation and extremely high RMSE. It is determined that the OK and SK algorithms not suitable for this dataset because of the difficulty of fitting the semivariogram model despite their lower RMSE and the higher RMSS.

Table 9. Comparison of prediction errors (Herring block)

Interpolation Method	RMSE	MSE
IDW	455.1	0.0714
Ordinary Kriging	452.7	-0.000218
Ordinary Kriging (Log)	718.6	0.0568
Simple Kriging	450.5	-0.003029
Indicator Kriging	452.9	0.067

Notes: RMSE: Root mean square error. MSE: Mean square error

4.3 Results

The reserves of Herring block (see Figure 15 for the location of Herring block) were calculated using the five interpolation methods. The tonnages of gold for Herring block at various cut-off grades are shown in Table 10. The tonnage estimated by OK-log is excluded in this table due to its extremely high RMSE and the tonnages almost double than those of other interpolation methods. It is deemed unsuitable for this dataset. For comparison purpose, the resource estimation was also calculated using the Thiessen polygons method.

Table 10. Tonnages of gold of Herring Block with various cut-off grades (Herring block)

Methods/ cur-off grade	Tonnage (Kg) of gold at various cut-off grade (mg/m³)							
cut-off grade (mg/m³)	0	200	400	600	800	1000	1200	1400
IK	5380	4761	2974	424				
IDW	5209	4482	2696	1336	749	438	294	200
OK	5353	4737	2869	710	124	2		
SK	5427	4993	2548	516				
Polygon	4999	4146	2999	2460	1868	1246	1079	923

At lower cut-off grade from 0 mg/m³ to 400 mg/m³, the tonnages estimated using various interpolation methods have significant difference (Figure 17), and the difference rapidly increases at higher cut-off grade. Thiessen Polygon method gets the higher tonnages at all cut-off grade levels up to 1400 mg/m³ and IDW has the second highest estimation. Krigings (OK, SK, IK) have no estimation above the cut-off grade of 800 mg/m³ due to the smoothing effect.

Zhou, W., Minnick M. D., and Cui, C. (2018) GIS for Natural Resources (Mineral, Energy, and Water). In: Huang, B. (Ed.), Comprehensive Geographic Information Systems Vol. 2, pp. 158–186. Oxford: Elsevier. ISBN: 9780128046609 https://doi.org/10.1016/B978-0-12-409548-9.09643-3

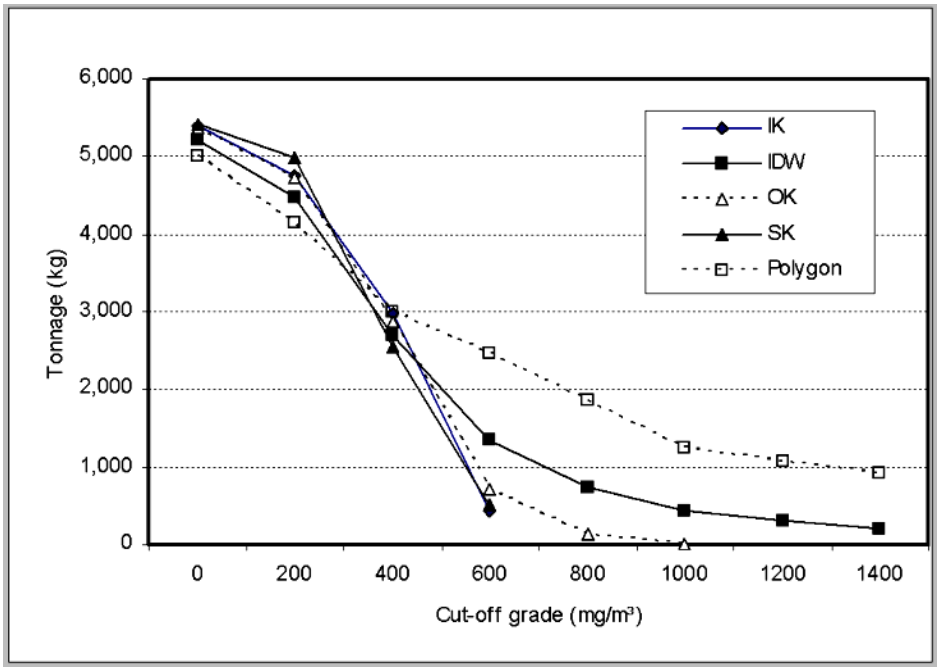

Figure 17. Tonnages of gold with various cut-off grades (Herring block) (Li et al., 2005)

4.4 Summary

Two databases were developed during this research, namely the IG and the R2.5DG. The IG is a data container which could be used for data management and information query, and the R2.5DG is capable of handling volume calculation, and resource estimation. A customized resource approach was built around this project, which can be used to estimate gold resources at different cutoff grades and different spatial domains in a time-efficient way. The geostatistical analysis in this case study has revealed that gold concentration dataset collected from the Nome offshore deposit are near lognormal distribution, positive skewed, directional, and has outliers. Inverse Distance Weighted (IDW), Ordinary Kriging (OK), Ordinary Kriging with lognormal transformation (OK-log), Simple Kriging (SK) and Indicator Kriging (IK) were assessed and compared with each other in the study. Cross-validation technique is employed to examine the accuracy of the five approaches. It is determined that the IWD and IK algorithm seem to provide estimations more agreeable with the conventional polygon method.

5.0 Conclusions

In this chapter we have demonstrated the comprehensive applications of GIS in natural resource analyses through three case studies. Natural resources embrace a broad category of various resources. We were only able to focus on a few, i.e. water, energy, and mineral resources. Natural resource analyses are by-nature spatial problems. The digital and geospatial capacities of GIS can bring the analyses to a new depth that was impossible or nearly impossible to achieve by the traditional ways. These in-depth

analyses presented in this chapter include:

(1) Managing a large amount of data in heterogeneous formats.
(2) Integrating geological data and information management.
(3) Constructing geospatial infrastructure as a central data repository and as a connector for various analytical models.
(4) Visualizing geospatial data in two-dimensional and three-dimensional.
(5) Enabling 3D geological or subsurface modeling.
(6) Quantitatively analyzing of groundwater vulnerability
(7) Interactively estimating total in-place mineral resource with different cut-off grades.

Traditional methods for natural resource analysis are very important. These methods collect first-hand of data and can not be replaced by any other means. The combination of traditional methods and GIS-based methods are essential parts for any natural resource analysis project. Traditional methods collect the first-hand data and GIS bring the analysis to a new depth in time-effective and cost-efficient fashion.

6.0 Acknowledgement

The Piceance Basin water for oil shale project was funded by US Department of Energy (Award # DE-NT0006554). The Florida groundwater vulnerability project was funded by the Florida Department of Health for funding this research through a subcontract with HAZEN and SAWYER, P.C. (JOB No.: 44237-001). The Nome placer gold GIS project was funded by the MMS (Minerals Management Services, U.S. Department of the Interior).

7.0 References

Articles in Journals

Arthur J. D., Wood H. A. R., Baker A. E., Cichon J. R. and Raines G. L. (2007). Development and implementation of a Bayesian-based aquifer vulnerability assessment in Florida. *Natural Resource Research* 16(2):93–107

Aspinall, R. and Pearson, D. (2000). Integrated geographical assessment of environmental condition in water catchments: Linking landscape ecology, environmental modeling and GIS, Journal od Environmental Management 59(4), 299-319

Berry P., Pistocchi A. (2003). A multicriterial geographical approach for the environmental impact assessment of open-pit quarries, International Journal of Surface Mining, *Reclamation and Environment* 17(4), 213-226

Barton L., McLay C. D. A., Schipper L. A. and Smith C. T. (1999). Annual denitrification rates in agricultural and forest soils: a review, *Australian Journal of Soil Research* 37, 1073–1093

Bronston, M. A. (1989). Offshore placer drilling technology - A case study from Nome, Alaska: *Mining Engineering* 42(1), 26-31

Cui, C., Zhou W., and Geza, M. (2016). GIS-based nitrogen removal model for assessing Florida's Surficial Aquifer vulnerability, *Environmental Earth Sciences* 75(6), 1-15

Di Luzio, M., Srinivasan, R., and Arnold, J. G. (2004) A GIS-coupled hydrological model system for the watershed assessment of agricultural nonpoint and point sources of pollution, *Transactions in GIS*, 8(1), 113-136

Dillon U., Blackwell G. (2003). The use of a geographic information system for open pit mine development, *CIM Bulletin* 96 (1069), 119-121

Hammond, A. D. (2002). GIS applications in underground mining, *Mining Engineering* 54(9), 27-30

Heatwole, K. K. and McCray. J. E. (2007). Modeling potential vadose-zone transport of nitrogen from onsite wastewater systems at the development scale. *Journal of Contaminant Hydrology* 91: 184-201

Jury, W. A., Focht, D. D. and Farmer, W. J. (1987). Evaluation of pesticide ground water pollution from standard indices of soil-chemical adsorption and biodegradation, *J. Environ. Qual.* 16, 4: 422-428

Li, H., Luo, H., Chen, G., **Zhou, W.**, and Huang S. L. (2005) Visualized Geostatistical Analysis of Nome Offshore Gold Placer Deposit Using ArcGIS – A Case Study, American institute of mining and metallurgical engineers transactions, Volume 318, 166-172

McCray, J. E., Kirkland, S. L., Siegrist, R. L. and Thyne, G. D. (2005). Model parameters for simulating fate and transport of on-site wastewater nutrients. *Groundwater* 43(4), 628-639

Rawls, W.J., Brakensiek, D. L. and Saxton, K. E. (1982). Estimation of soil water properties. *Transaction of American Society of Agriculture Engineering* 25(5), 1316-1320

Rivett, M.O., Buss, S. R., Morgan. P., Smith, J. W. and Bemment, C. D. (2008). Nitrate attenuation in groundwater: A review of biogeochemical controlling processes. *Water Research* 42, 16: 4215-4232

Schlosser, S. A., McCray, J. E., Murray, K. E. and Austin, B. (2002). A subregional-scale method to assess aquifer vulnerability to pesticides. *Ground Water* 40(4), 361-367

Wilson J. P., Mitasova, H. and Wright D. J. (2000), Water resource applications of Geographic Information Systems. *Urban and Regional Information System Association Journal*, 12(2), 61-79

Witheetrirong, Y., Tripathi, N. K., Tipdecho, T. and Parkpian, P. (2011). Estimation of the effect of soil texture on nitrate-nitrogen content in groundwater using optical remote sensing. *International Journal of Environmental Research and Public Health* 8(8), 3416-3436

Zhou, W., Chen, G., Li, H., Luo, H., and Huang, S. L. (2007). GIS application in mineral resource analysis – a case study of offshore marine placer gold at Nome, Alaska. *Computers and Geosciences* 33, 773–788

Zhou, W., Minnick, M. D., Mattson, E. D., Geza, M. and Murray, K. E. (2015). GIS-based geospatial infrastructure of water resource assessment for supporting of oil

shale development in Piceance Basin of northwestern Colorado. *Computers and Geosciences*, 77, 44–53

Books

Bonham-Carter, G. F. (1996). Geographic information systems for geoscientists – modeling with GIS. Tarrytown, N. Y., Pergamon, Elsevier Science Ltd., Computer Methods in the Geosciences, vol. 13, 1st ed. 1994, reprint in 1996. 398p.

Date, C. J. (2003). An introduction to database systems, 8th edition, Addison Wesley 1024p.

Fisher, N. I., Lewis, T. and Embleton, B. J. J. (1987). Statistical analysis of spherical Data, Cambridge University Press, 329p.

Jury, W. and Horton, R. (2004). Soil physics. New York. John Wiley & Sons, 384p.

Litton, G. (1987). Introduction to database management: a practical approach, William C Brown Pub, 532p.

Maidment, D.R. (2002) ArcHydro – GIS for water resources, 1st ed. ERSI Press, Redlands, California, 208p.

Navathe, S. B. and Elmasri, R. (2002). Fundamentals of database systems, 3rd Edition, Addison Wesley Longman, 1000p.

Ramesh Reddy, K. and Delaune, R.D. (2008). Biochemistry of wetlands: science and application. Boca Baton, FL: CRC Press 800p.

Wing, M.G. and Bettinger, P. (2008). Geographic information systems: Applications in natural resource management. Oxford University Press, Oxford. 272p.

Edited Books

Garnett, R. H. T. (2000). Marine placer gold, with particular reference to Nome, Alaska. In: David S. Cronan, (Ed), Handbook of Marine Mineral Deposits, CRC Press, 67-101

Naiman, R.J., Bisson, P.A., Lee, R.G., and Turner, M.G. (1997). Approaches to management at the watershed scale. In: Kathryn A. Kohm, and Jerry F. Franklin (Eds.), Creating a Forestry for the 21st Century: The Science of Ecosystem Management, Washington, DC: Island Press, 239-253

Zhou, W. (2009). An outlook of GIS applications in mineral resource estimation. In: Melanie D. Corral and Jared L. Earle (Eds) "Gold Mining: Formation and Resource Estimation, Economics and Environmental Impact", Nova Science Publishers, Inc. New York, 33-62

Reports and Theses

Anderson D. L. and Otis, R. J. (2000). Integrated wastewater management in growing urban environments. In: Managing soils in an urban environment. Agronomy Monograph 39. American Society of Agronomy, Crop Science Society of America, Soil Science Society of America

Beach, D. N. (2001). Infiltration of wastewater in columns. M.S. thesis. Colorado School of Mines, Golden, CO

Bronston, M. A. (1990). A view of sea-floor mapping priorities in Alaska from the mining industry: C1052, US Geological Survey Reports on Alaska Released in 1991, 1990, 86-91

Bundtzen, T. K., Reger, R. D., Laird, G. M., Pinney, C. S., Clautice K. H., Liss S. A., & Cruse, G. R. (1994). Progress report on the geology and mineral resources of the Nome Mining District, Division of Geological & Geophysical Surveys, Public-Data File 94-39

Cashion, W. B., and Donnell, J. R. (1972) Chart showing correlation of selected key units in the organic-rich sequence of the Green River Formation, Piceance Creek Basin, Colorado, and Uinta Basin, Utah: U.S. Geological Survey Oil and Gas Investigations Chart OC-65.

Chen, G., Huang, S. L. and Zhou, W. (2003). GIS applications to Alaskan near-shore marine mineral resources, stage II: enhancement of web site; improvement of GIS structure; predictive model development; and new site identification and study, an unpublished report to Minerals Management Services, U.S. Department of the Interior by University of Alaska Fairbanks, 45p.

Chen, G., Zhou, W., Huang, S. L., Li, H. and Luo, F. (2005). GIS applications to Alaskan near-shore marine mineral resources (phase III), an unpublished report to Minerals Management Services, U.S. Department of the Interior by University of Alaska Fairbanks, 159p.

Cui, C. (2014). GIS-Based nitrogen removal model for assessing Florida's Surficial Aquifer vulnerability from onsite wastewater treatment systems (Master's thesis). Colorado School of Mines, 86p.

Fischer, E. (1999). Nutrient transformation and fate during intermittent sand filtration of wastewater. M.S. thesis. Colorado School of Mines, Golden, CO

Hail, W. J., and Smith, M. C. (1994). Geologic map of the northern part of the Piceance Creek Basin, northwestern Colorado, U.S. Geological Survey Miscellaneous Investigations Series Map I-2400.

Hail, W. J., and Smith, M. C. (1997), Geologic map of the southern part of the Piceance Creek Basin, northwestern Colorado, U.S. Geological Survey Miscellaneous Geologic Investigations Map I-2529.

Huang, S. L., Chen, G., Maybrier, S. and Brennan, K. L. (2001). GIS applications to Alaskan near-shore marine mineral resources, an unpublished report to Minerals Management Services, U.S. Department of the Interior by University of Alaska Fairbanks, 280p.

Koschmann, A. H., and Bergendahl, M. H. (1968). Principal gold-producing areas of the United States, Geological Survey Professional Paper, 610p.

Mattson, E. D., Hull, L., Cafferty, K. (2012). Water usage for in-situ oil shale retorting – a system dynamic model, Idaho National Laboratory Report, Report No. INL/EXT-1227365

Mercier, T.J., Brownfield, M.E., Johnson, R. C., and Self, J. G.,(2009) Fischer assays of oil shale drill cores and rotary cuttings from the Piceance Basin, Colorado-2009 Updatep. 16, USGS Open-File Report 98-483 Version2.

McCray, J. E., Geza, M., Lowe, K., Tucholke, M., Wunsch, A., Roberts, S., Drewes, J., Amador, J., Atoyan, J., Kalen, D., Loomis, G., Boving, T. and Radcliffe, D. (2010). Quantitative tools to determine the expected performance of wastewater soil treatment units: guidance manual. Water Environment Research Foundation. Alexandria, 198p.

National Research Council (1999). New strategies for America's watersheds, Washington, DC: National Academy Press, 328p.

Nelson, C. H. and Hopkins, D. M. (1972). Sedimentary processes and distribution of particulate gold in the Northern Bering Sea, Geological Survey Professional Paper 689

NETL (National Energy Technology Laboratory, U.S. Department of Energy) (2007) Oil shale environmental issues and needs workshop report 61p.

Price, M. J. (2001). Geographic information systems and industrial minerals, preprint 01-116, Society of Mining Engineers

Tagg, A. R. and Greene, H. G. (1973). High-resolution seismic survey of an offshore area near Nome, AK: Geological Survey Professional Paper 759-A

USGS (2005). Geology and resources of some world oil-shale deposits, USGS Scientific Investigations Report 2005–5294

Youssef, M. A. (2003). Modeling nitrogen transport and transformations in high water table soils. Doctoral dissertation. North Carolina State University, Raleigh, NC

Zhou, W., Minnick, M. D., Geza, M., Murray, K. E. and Mattson, E. D. (2012). GIS- and web-based water resources geospatial infrastructure for oil shale development, the Final Project Report to United States Department of Energy, National Energy Technology Laboratory, December 29, 2012, Report No. DOE/NT0006554-1, 143p.

Conference Symposiums

Luo, H., Li, H., Chen, G., Zhou, W. and Huang, S. L. (2005). Application of web GIS for Nome Alaska offshore mineral resource management and utilization, the *Proceedings of 2005 Society for Mining, Metallurgy, and Exploration (SME) Annual Meeting*, February 28 - March 2, Salt Lake City, Utah, 2005

Rao, P. S. C., Hornsby, A.G. and Jessup, R.E. (1985). Indices for ranking the potential for pesticide contamination of groundwater. *Soil Crop Science Society Florida Proceedings* 44, 1-8

Electronic Media

Almarales–Hamm, D.; Campos, G. D.; Murray, B. and Russell, N. (undated) The application of GIS to bauxite mining in Jamaica, access date: August 2005, URL: http://www.esri.com/mapmuseum/mapbook_gallery/volume19/mining7.html

Brownfield, M. E., Self, J. G. and Mercier, T. J. (2011), Fischer assay histograms of oil-shale drill cores and rotary cuttings from the Great Divide, Green River, and Washakie Basins, Southwestern Wyoming, USGS Digital Data Series DDS-69-DD, 9p.

EarthSTEPS, LLC and GlobalMind (2009) Statewide inventory of onsite sewage treatment and disposal systems in Florida. Final Report prepared for the Florida Department of Health. access date: December 12, 2013. URL: http://www.floridahealth.gov/healthy-environments/onsite-sewage/research/_documents/research-reports/_documents/inventory-report.pdf.

ESRI (2003). Using ArcGIS Geostatistical Analyst, ESRI (Environmental Systems Research Institute, Inc.) Digital Book, 306p.

ESRI (2004a). Building a geodatabase, ESRI (Environmental Systems Research Institute, Inc.) Digital Book, 382p.

ESRI (2004b). Using Spatial Analyst, ESRI (Environmental Systems Research Institute, Inc.) Digital Book, 232p.

ESRI (2006). GIS best practices for mining, Access Date: August 2006, URL: http://www.esri.com/industries/mining/business/literature.html

Florida Department of Environmental Protection (undated), access date: February 24, 2017, URL: http://www.dep.state.fl.us/swapp/Aquifer_Pframe.html

Florida Department of Health (2014) Onsite sewage, access date: January 30, 2014, URL: http://www.floridahealth.gov/healthy- environments/onsite-sewage/index.html

Johnson, R. C., Mercier, T. J., Ryder, R. T., Brownfield, M. E. and Self, J. G. (2011) Assessment of in-place oil shale resources of the Eocene Green River Formation, Greater Green River Basin, Wyoming, Colorado, and Utah, USGS Digital Data Series DDS-69-DD, 68p.

Mercier, T. J., Brownfield, M. E. and Johnson, R. C. (2011a). Methodology for calculating oil shale resources for the Green River and Washakie Basins, Southwestern Wyoming, USGS Digital Data Series DDS-69-DD, 52p.

Mercier, T. J., Gunther, G. L. and Skinner, C. C. (2011b). The GIS project for the geologic assessment of in-place oil shale resources of the Eocene Green River Formation, Greater Green River Basin, Wyoming, Colorado, and Utah, USGS Digital Data Series DDS-69-DD, 5p.

Mercier, T. J. (2011) Calculation of overburden above the LaClede ed of the Laney Member of the Eocene Green River Formation, Green River and Washakie Basins, Southwestern Wyoming, USGS Digital Data Series DDS-69-DD, 10p.

Self, J. G., Johnson, R. C., Brownfield, M.E., and Mercier, T. J. (2010) Simplified stratigraphic cross sections of the Eocene Green River Formation in the Piceance Basin, Northwestern Colorado p.7, USGS Digital Data Series DDS–69–Y, Chapter 5

Self, J. G., Ryder, R. T., Johnson, R. C., Brownfield, M. E. and Mercier, T. J. (2011) Stratigraphic cross sections of the Eocene Green River Formation in the Green River Basin, Southwestern Wyoming, Northwestern Colorado, and Northeastern Utah, USGS Digital Data Series DDS-69-DD, 11p.

USGS (2007). Geographic information systems, access date: February 22, 2007, URL: http://erg.usgs.gov/isb//pubs/gis_poster/

Wood, T., Dammer, A., Wilson, C., Parker, J., Skaggs, R. and Stovall, T. (2008). An overview of the water management cross-cut plan for commercialization of America's unconventional fuels, In: J. Boak and H. Whitehead, (Eds) Proceedings of the 27th Oil Shale Symposium, Colorado Energy Research Institute Document 2008-1, Colorado School of Mines. Golden CO USA (CD-ROM)

Zhou, W., Minnick M. D., and Cui, C. (2018) GIS for Natural Resources (Mineral, Energy, and Water). In: Huang, B. (Ed.), Comprehensive Geographic Information Systems Vol. 2, pp. 158–186. Oxford: Elsevier. ISBN: 9780128046609 https://doi.org/10.1016/B978-0-12-409548-9.09643-3